UNITED STATES NAVAL POSTGRADUATE SCHOOL

THESIS

CATIONIC PERTURBATIONS OF SPIN DENSITIES IN ANION FREE RADICALS

by

James Kenneth Poole

May 1966

CATIONIC PERTURBATIONS OF SPIN DENSITIES IN ANION FREE RADICALS

by

James Kenneth Poole
Lieutenant, United States Navy
B. S., United States Naval Academy, 1959

Submitted in partial fulfillment
for the degree of

MASTER OF SCIENCE IN CHEMISTRY

from the

UNITED STATES NAVAL POSTGRADUATE SCHOOL

May 1966

Signature of Author James K. Poole
Weapons Sys Engr Curriculum, May, 1966

Certified by William M. Tolles
Thesis Advisor

Accepted by: G. F. Kinney
Chairman, Department of Material Science and Chemistry

Approved by: R. F. Rinehart
Academic Dean

ABSTRACT

In an investigation of cationic perturbations of spin densities in anion free radicals, as disclosed by variations in proton coupling constants, the EPR spectra of anion free radicals of benzophenone, biphenyl, anthracene, terephthalonitrile and hexacyanobenzene were observed. Radicals were prepared in vacuo, using a vacuum electrolytic cell and/or sodium reductions in tetrahydrofuran solution. The spectra of the anthracene and terephthalonitrile radicals, prepared by reduction with sodium in tetrahydrofuran, displayed sodium splitting. It was observed that the coupling constants for protons and nitrogens in the terephthalonitrile radical were smaller in the presence of sodium ion than in the presence of tetra-n-butyl ammonium perchlorate.

It was observed that the addition of tetra-n-butyl ammonium perchlorate to sodium-reduced solutions of anthracene or terephthalonitrile removed the sodium coupling, giving narrow-line EPR spectra identical with those obtained by electrolysis in vacuo.

Coupling constants for the radicals were determined by a least-squares analysis of the envelope of the central portion of the spectrum, marking field intervals with an NMR field-tracking gaussmeter and utilising a computer program which synthesises an EPR spectrum when given coupling constants and other parameters.

This research was carried out at the U. S. Naval Postgraduate School, Monterey, California.

TABLE OF CONTENTS

LIST OF TABLES

LIST OF ILLUSTRATIONS

TABLE OF SYMBOLS AND ABBREVIATIONS

Symbols

$\mathbf{A}$	hyperfine coupling tensor
Å	Angstrom, 10^{-8} cm
C_{ij}	coefficients of LCAO-molecular orbitals, Ψ_j
E	energy
H	applied magnetic field
H^o	static magnetic field
H_o	alternating magnetic field
H_{rr}	Coulomb integral,
H_{ro}	bond integral,
$\mathcal{H}$	the Hamiltonian operator
$\vec{I}$	nuclear spin
$\vec{J}$	spin angular momentum
K	empirical constant in formula (3-34); also, effective "Q" for nitrogen splittings in (3-38)
K_{eq}	equilibrium constant
$\vec{L}$	torque
$\vec{M}$	total magnetic moment
$N_{\pm}$	nuclear energy level populations for I = 1/2
$N_{\pm}^o$	steady state values of $N_{\pm}$
P	perturbation strength
Q	McConnell's Q, from (3-33)
$\vec{S}$	electron spin

S_{rs}	overlap integral
T	temperature, ^{o}K
T_1	spin-lattice (longitudinal) relaxation time
T_2	spin-spin (transverse) relaxation time
$W_{+/-}$	probability per second of a spin transition from state m = + 1/2 to - 1/2; $W_{-/+}$ for reverse
W	spin transition probability for $W_{+/-} = W_{-/+}$
W_u	transition probability (m = + 1/2 to m = - 1/2) for spin system coupled to reservoir; W_d for reverse
a_H	proton coupling constant
a_N	nitrogen coupling constant
c	speed of light = 3×10^{8} m/sec
e	charge on the electron = 1.6×10^{-19} Coulomb
$\overline{\overline{g}}$	spectroscopic splitting tensor
$\hbar$	Planck's constant/2π = 1.05×10^{-27} erg-sec
h_X	correction factor for Coulomb integral of heteroatom X
k	Boltzmann's constant = 1.38×10^{-23} Joule/^{o}K
k_{CX}	correction factor for bond integral of a C-X bond
m	electron mass = 9.1×10^{-31} kg
n	population difference, $N_+ - N_-$
n_o	value of n at t = 0
n_s	steady state value of n
α	positive electron spin; also, Coulomb integral H_{rr}
β	negative electron spin; also, bond integral H_{rs}; Bohr magneton
β_N	nuclear magneton

γ	gyromagnetic ratio for electron
γ_N	gyromagnetic ratio for nuclei; $\gamma/2\pi$ = 4.25759 kc/gauss for protons
Δ	change in
ϵ	excess charge density on a C-H bond
θ	angle
λ	eigenvalues
μ_e	electron magnetic moment
μ_N	nuclear magnetic moment
ν	frequency, cps
ρ	electron density
τ	coordinates for integration over "all space"
ϕ_i	$2p_z$ atomic orbital for atom i
ϕ_π	wave function for all pi electrons in a molecule
χ	magnetic susceptibility
χ'	magnetic susceptibility, real part
χ''	magnetic susceptibility, imaginary part
ψ_o	ground state electronic wave function for a molecule
ψ_j	two-electron molecular orbitals, combinations of $2p_z$ atomic orbitals
ω, Ω	angular velocity, radians/sec

Abbreviations

DEE	diethyl ether
DME	1, 2 dimethoxyethane
DMF	N,N-dimethylformamide

DMSO	dimethylsulfoxide
DPPH	α,α-diphenyl-β-picrylhydrazyl
EPR	electron paramagnetic resonance
NMR	nuclear magnetic resonance
PBSQ	para-benzosemiquinone
TBAB	tetra-n-butylammonium bromide
TBAP	tetra-n-butylammonium perchlorate
THF	tetrahydrofuran
THP	tetrahydropyran
TMED	tetramethylenediamine

1. Introduction

The phenomenon of electronic paramagnetic resonance (EPR)[1] was introduced in 1945 by the observation of a resonant absorption of radio-frequency energy in a sample of crystalline $CuCl_2 . 2H_2O$ in a magnetic field;[2] two years later, the spectrum of the free radical pentaphenyl-cyclopentadienyl, $(C_6H_5)_5C_5$, was obtained.[3] Many other stable organic free radicals were soon studied, including α,α-di-phenyl-β-picrylhydrazyl (DPPH) [4] , various semiquinone anions [12] , triphenyl-methyl [9] , and the cation or anion radicals of assorted aromatic hydrocarbons [28] . Hyperfine structure was resolved in the spectra, and appeared to be due to the interactions of the unpaired electron with the protons in the rings or on substituent alkyl groups. McConnell [19] , [23] postulated that the hyperfine coupling constant, a_H, of a particular ring proton in an aromatic system is proportional to the unpaired pi-electron density, ρ_C, at the carbon atom to which it is attached, i.e.,

$$a_H = Q\rho_C, \tag{1-1}$$

where Q is a proportionality constant with the value of about 23 gauss.

---

1. The term EPR will be used in preference to "electron spin resonance", as it refers to the magnetic resonance of the permanent magnetic moments of electrons, and contributions from both orbital angular momentum and spin angular momentum must be considered for these magnetic moments. [85]

2. E. Zavoisky, J. Phys. USSR 9, 211, 245 (1945); cited in [14] .

3. B. M. Kozyrey and S. G. Salikhov, Doklady Akad. Nauk. S.S.S.R. 58, 1023 (1947): cited in [14] .

Much of the early work was done with the anion radicals which resulted from the reduction of various aromatic compounds by alkali metals in dry, oxygen-free ethereal solvents. Due to the observation of cation-dependent shifts in the absorption bands of their optical spectra [22], [59], such solutions had been presumed to contain ion-pairs in equilibrium with dissociated species; thus, the discovery of further hyperfine splitting of the well-interpreted EPR spectrum of naphthalene anion radical by sodium ion (I=3/2) in tetrahydrofuran [53] was not too surprising. In this study, the sodium coupling constant was found to vary appreciably with temperature and solvent used, but the couplings observed for the two sets of equivalent protons were invariant within experimental error (3%). Hush and Rowlands [106] calculated the energies of absorption bands of the anion radicals of anthracene and napthalene in the presence of various alkali metal cations, using a simple perturbation treatment. They suggested that potassium caused such band shifts in napthalene without causing hyperfine splitting in the EPR spectrum because the hyperfine interaction constant for potassium is much smaller than that for sodium. Absorption band shifts were observed for anthracene, although alkali metal splitting had not been observed in the EPR spectra of this radical.

The search for better resolution of hyperfine structure led to electrolytic reduction, which offered the advantages of controlled reaction and elimination of alkali metal ions from the solution. Aprotic solvents of relatively high dielectric constant and bulky (tetra-alkyl

ammonium) counter-ions were used to minimize the complicating effects of ion association. Austen, et al., reduced anthracene, benzophenone and anthraquinone electrolytically, observing the EPR spectra of the radicals in frozen N, N-dimethyl formamide (DMF) solutions [27]. Soon after, Maki and Geske observed the EPR spectra of the electrolytically-generated anion radicals of several nitro compounds at room temperature in acetonitrile solution. [40], [43], [58]

In comparing the spectra of some radicals in different environments, differences became apparent; aside from variations or absence of alkali metal couplings, changes were noted in the proton hyperfine coupling constants. Stone and Maki observed variations of up to 45% in the values of proton coupling constants of semiquinones generated by electrolysis of quinones in aprotic solvents, as compared with values for radicals prepared in alkaline aqueous and/or alcoholic solutions. [90]

Further variations of coupling constants (for protons, N^{14}, or C^{13}) with solvent characteristics were noted for radicals of thioindigo [82], aromatic and aliphatic-substituted nitric oxides [110], para-substituted nitrobenzenes [110], [138], [95], fluorenone [134], [96], meta-nitrophenol [121], nitrobenzene [120], biphenyl [135], semiquinones [141], [152], and benzophenone [96].

Gendell, Freed and Fraenkel [80] have published a theoretical discussion of solvent effects, in which the solvent dependence of hyperfine splittings is shown to result from a redistribution of the pi-electron spin density, such redistribution being due to localized complexes between the solvent and polar substitutents or heteroatoms in the radical

molecule.

Examples of counter-ion dependent coupling constants have been reported for benzophenone [69] , [83] , ortho-semi-quinones [124] , para-chloronitrobenzene [131] , anthracene [118] , pyracene [122] and azulene. [136]

Reddoch [149] has published a rather complete study of the dependence of the proton coupling constants of anthracene and azulene anion radicals on solvent, cation, concentration and temperature. He attributes the variations in coupling constants to ion-pair formation, even when alkali-metal splitting is not observed, and calculates the effect of the associated cation on the coupling constants of the anion.

The objective of the present study was to develop methods of introducing progressively increasing counter-ion perturbations of the electron spin density distributions in anion free radicals, observe any resulting shifts in proton coupling constants, and determine what mathematical treatment was required to produce similar shifts in the electron densities calculated by molecular orbital theory.

2. Experimental Methods

Spectrometer

All EPR spectra were taken on a Varian V-4502-13 EPR Spectrometer with Fieldial V-FR 2503 magnetic field regulation and a nine inch magnet, using 100 kc modulation. Spectra were recorded on a Moseley AUTOGRAF X-Y recorder, Model 2S.

Materials

Tetrahydrofuran (THF) was used as the solvent in the preparation of all radicals investigated, both by alkali metal reduction and electrolysis. THF appeared to be a good choice, since it was volatile enough to be easily purified in a vacuum system and has been noted to permit the formation of ion-pairs between radical anions and cations present without reacting with either. Bolton and Fraenkel give a brief discussion of the merits of some solvents commonly used in electrolytic generation of free radicals. [118]

THF (Eastman White Label) was purified by distillation over calcium hydride under a nitrogen atmosphere, then stored in glass-stoppered bottles until use. A large (4 mm diameter, 20 mm deep) solvent storage bulb was attached permanently to a greaseless vacuum line, flushed with nitrogen, and loaded with 10-30 ml of a 0.2 molar THF solution of sodium benzophenone ketyl which had been prepared under nitrogen and allowed to react for several days. After degassing this solution by repeated freezing, pumping and melting, pure THF could

be distilled off under vacuum. To replenish the solvent, the previously distilled THF was treated with $LiAlH_4$ until escaping H_2 could no longer be detected, degassed on the vacuum line, and vacuum distilled into the solvent storage bulb. (The solvent supply was usually replenished before the solution in the storage bulb became noticeably viscous, to prevent violent "bumping" of the solution during the vacuum distillations.) As long as the purple or blue color of the radical in the bulb persisted, the solvent could be assumed free from water, oxygen, carbon dioxide, or other impurities which would destroy the radical.

Initially, Apiezon M stopcock grease was used in the vacuum system; Kel-F was used in a later system, until it was noted that THF distilled through this system appeared to consistently prevent the formation of radicals or cause their rapid decay. THF seemed to be absorbed by the grease, making it almost impossible to pump the system down after a distillation had been carried out. To eliminate the possibility of the solvent interacting with stopcock grease, a "greaseless" section of vacuum line was added to the system, (including solvent storage bulb and connection joints) using Fischer and Porter 4 mm Telflon needle valves throughout. These valves were quite satisfactory, although the Viton A O-rings dissolved in THF and had to be replaced frequently because of wear.

Benzophenone (Eastman White Label) was recrystallized twice from anhydrous ethyl alchol (U. S. Industrial Chemicals Co.) and stored in a vacuum desiccator over silica gel. Anthracene (Fisher Scientific

Company) was purified by sublimation. Terephthalonitrile (Eastman White Label), biphenyl (Eastman White Label), hydroquinone (Fisher Scientific Company) and hexacyanobenzene [4] were used unpurified.

Following the example of Bolton and Fraenkel [18], tetra-n-butyl ammonium perchlorate (TBAP) was chosen as the supporting electrolyte, since the lower tetra-alkyl ammonium compounds such as tetra-propyl ammonium perchlorate are not very soluble in THF. Tetra-alkyl ammonium salts have been used as electrolytes in a number of ESR studies; they do not appear to react with the radicals produced, provide any extra nitrogen splittings, or affect the coupling constants appreciably as their concentration is varied. They appear to be stable under electrolytic conditions, although short-lived perchlorate radicals have been observed during in situ electrolyses of lithium, sodium and silver perchlorates in acetonitrile. [35]

Tetra-n-butyl ammonium perchlorate (TBAP) was prepared as suggested by Luder, et al. [1] Tetra-n-butyl bromide (TBAB) (Eastman White Label) and $AgClO_4$ (G. F. Smith Chemical Company) were dissolved in separate portions of 95% ethyl alcohol, then mixed slowly with stirring. After standing overnight to allow the colloidal AgBr to coagulate, the solution was filtered through fritted glass and evaporated

---

[4] A small sample of hexacyanobenzene was kindly provided by Dr. Peter Hammond of the U. S. Naval Ordnance Test Station, China Lake, California.

to leave crystalline TBAP. The resulting product was recrystallized twice from anhydrous ethyl acetate (Baker and Adamson).

Most of the TBAP actually used was obtained from Southwestern Analytical Chemicals, Inc., and recrystallized twice from anhydrous ethyl acetate; a later supply was obtained from Matheson, Coleman and Bell.

Field Calibration

To observe small shifts in coupling constants, it was anticipated that precise, reproducible measurements of differences in magnetic field would be required. Varian Associates state that the automatic sweep provided with the Fieldial accessory is linear to within 0.5%, however, calibration is advisable. The field sweep was calibrated using para-benzosemiquinone (PBSQ) prepared according to the method of Venkataraman, et al. [13] (Five mg of hydroquinone was dissolved in 1.5 ml 95% ethyl alcohol, then allowed to oxidize in the air after addition of a pellet of NaOH.) PBSQ gives a spectrum of five lines, equally spaced at 2.368 $\pm$ .001 gauss [37] ; the actual scale of gauss per inch could be determined by measuring the coupling constants from an experimental spectrum, and the linearity of the sweep checked by comparing the measured splittings at high, intermediate and low fields, shifting the whole spectrum by changing field settings for sweeps greater than ten gauss. With this method, detection of small non-linearities was limited by the probable error of measurement (0.01 inch).

Better results were obtained using a magnetic field-tracking nuclear magnetic resonance gaussmeter (hereafter referred to as "NMR Gaussmeter") constructed by Mr. R. A. Sanders. A radio-frequency marginal oscillator similar to that described by Pound and Knight [5] was referenced to the NMR frequency of a 1.0 M $CuSO_4$-doped H_2O sample placed adjacent to the EPR cavity in the field. A feedback system similar to that of Maki and Volpicelli [147] permitted the oscillator to "track" the NMR frequency as the magnetic field was changed; the oscillator frequency was monitored with a Hewlett-Packard 524 frequency counter (10-100 Mc), and markers applied manually to the EPR spectrum at convenient intervals by means of a simple circuit which introduced a step input to the Y-axis of the recorder when the button was pushed.

When working with previously observed spectra, accurate values of the coupling constants could be obtained by taking repeated counter readings at the centers of selected strong, non-overlapping lines of the spectrum. These lines were chosen by drawing a "stick diagram" using the expected coupling constants, as in Figure 1 (b) for anthracene.

Electrolytic Reduction - Apparatus and Procedures

Electrolytic reduction was chosen to obtain the advantages of complete, controlled reaction in the absence of the complicating splittings of alkali metal cations. Many electrolysis cells have been designed for use inside the microwave cavity [40], since this plan offers simplicity and ease of operation; inert gas atmospheres, flow systems,

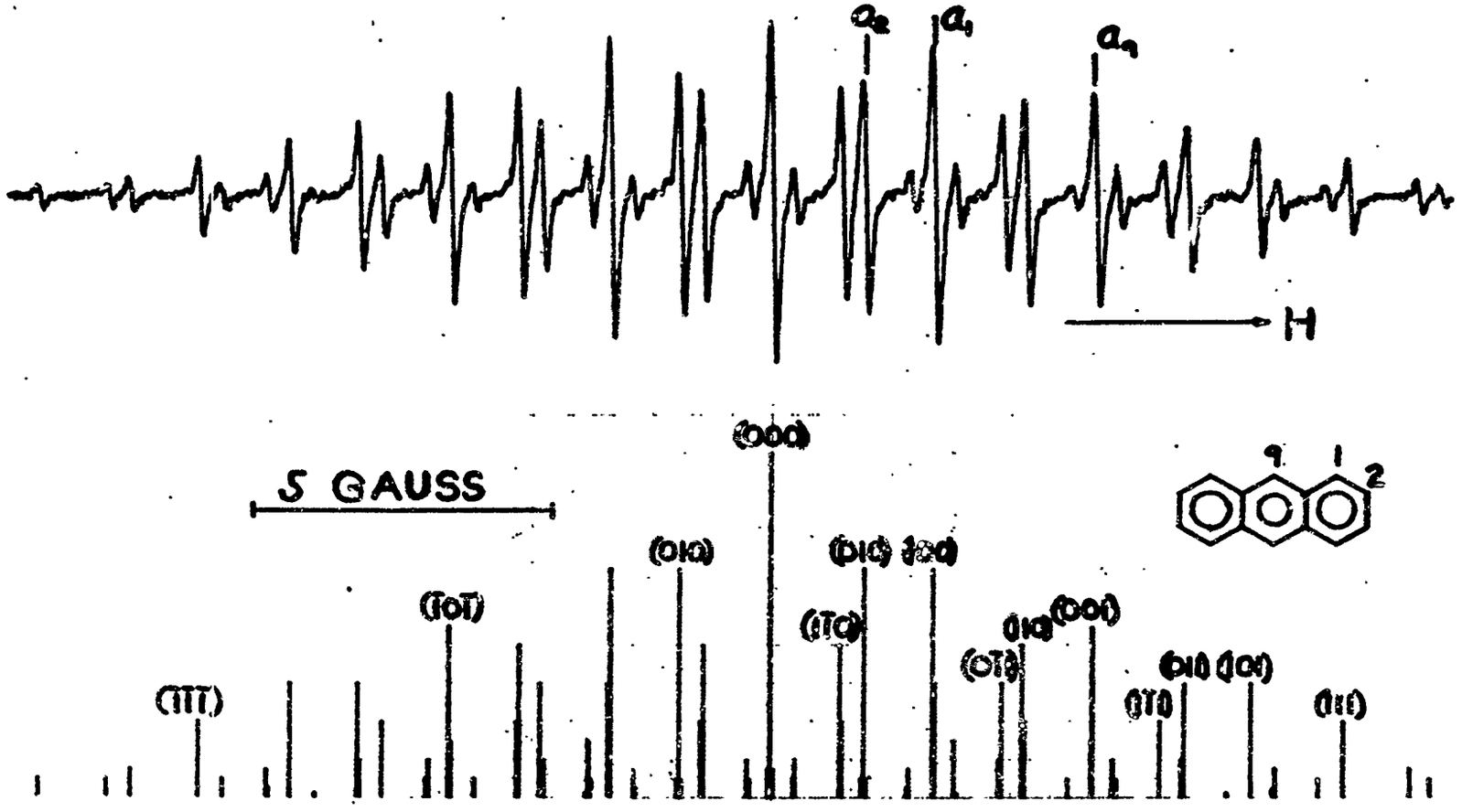

Figure 1 (a). Experimental EPR spectrum of anthracene anion radical, prepared by reduction with sodium in the presence of excess TBAP.

(b). Positions and intensities of lines, reconstructed from experimental coupling constants for anthracene.

etc., may easily be employed.

It was decided to build an electrolytic cell which would be operated outside the cavity, following the example of Rieger, et. al. [112]; this required the transfer of prepared radical solutions to the cavity, but had the advantage that the cell and electrodes could be made large enough to allow rapid and quantitative reduction of the sample. (Complete reduction is usually required if acceptably narrow lines are to be obtained, as many radicals undergo rapid electron exchange reactions with unreduced species which broaden the spectral lines.) The use of a large cell permits more precise measurement of the amount of material used and number of coulombs passed during the electrolysis, thus better control of reductions should be possible. An external cell also permits the observation of color changes, bubbling. etc., as the reaction proceeds.

Complete exclusion of radical-destroying impurities such as 0_2, CO_2, H_20, etc, ean only be approached by using vacuum techniques; accordingly, a vacuum electrolytic cell was constructed according to a design adapted from that of Bolton and Fraenkel. [118] (See Figure 2) A possible disadvantage of this system is the use of standard taper joints, requiring ample use of stopcock grease for sealing. Johnson and Chang [14] have recently employed a simplified version of the Bolton-Fraenkel design, using 0-ring joints and Teflon stopcocks throughout to make the system completely greaseless; this should be a great improvement, provided the solvent is not allowed to come in

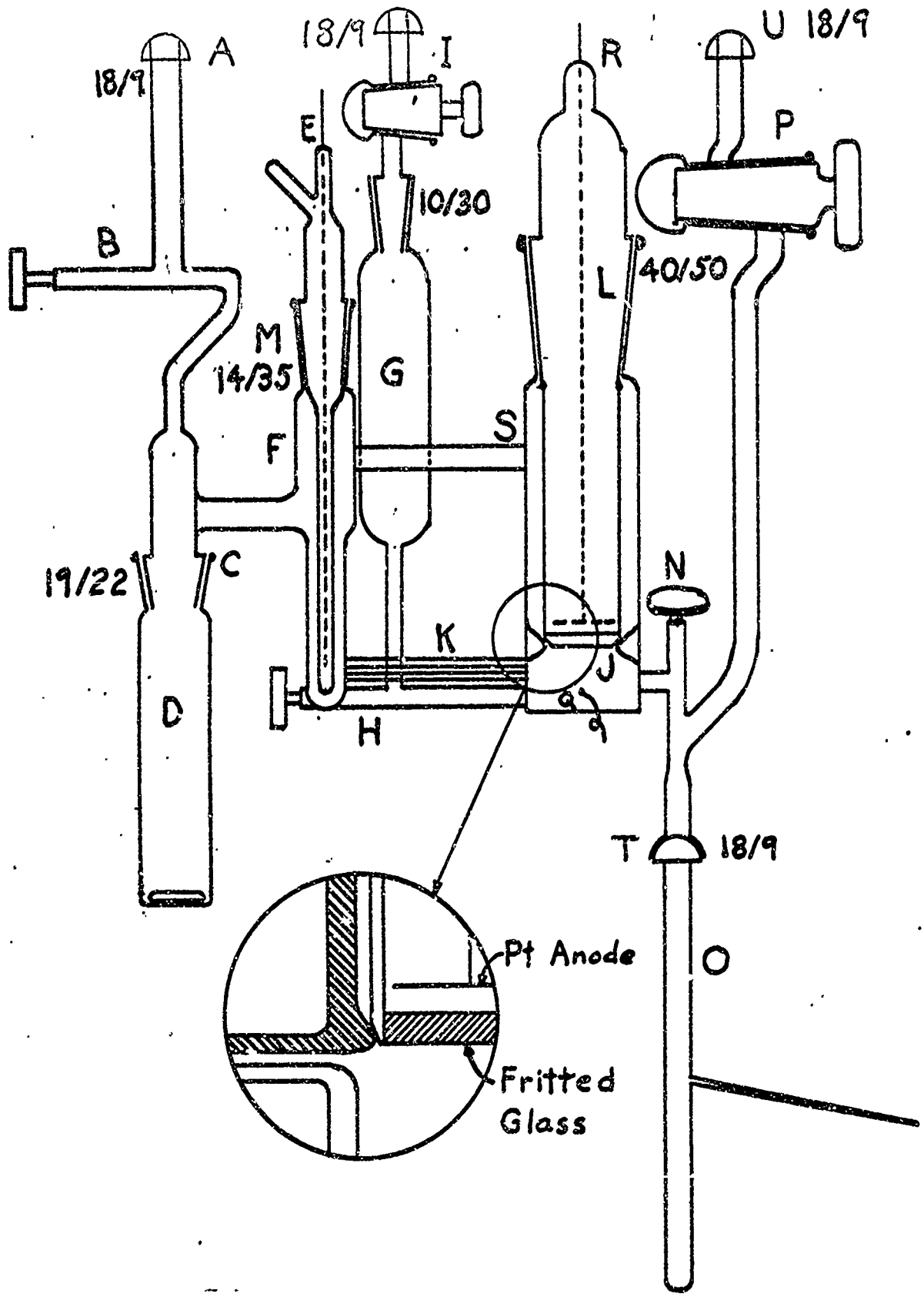

Fig. 2. Vacuum Electrolytic Cell.

contact with the O-rings.

For descriptive purposes, the cell may be divided into the following sections: mixing chamber D, reference electrode E, reference compartment F, mercury storage bulb G, cathode compartment J, anode compartment L. Valves B, H and N are 1 mm Teflon-glass needle valves (Fischer and Porter). These valves are also available in a 4 mm size, which could be used to provide greater strength and faster evacuation of the cell while retaining adequate control of liquids. A small magnetic stirrer, made by fusing glass tubing around a short length of steel drill rod, was used in the mixing chamber to expedite the mixing process. The reference electrode consisted of a silver wire in a 0.1M solution of $AgClO_4$ in dimethylsulfoxide (DMSO), enclosed in a glass tube. The tip of the tube (4 mm o.d.) was fused about a small asbestos fiber, then ground on emery until the resistance of the electrode (when filled with saturated KCl solution) was 4-5 Mohms. The silver wire was spot welded to a tungsten wire sealed through the glass at E. A very small pinhole was "punched" in the electrode just below joint M by evacuating it and subjecting it to the discharge of a Tesla coil; this permitted the reference electrode to be evacuated with the rest of the apparatus, preventing the electrolyte from being forced through the asbestos into the reference compartment. Too large a pinhole, however, permitted excessive DMSO to effuse, making it difficult to achieve the required vacuum. The mercury storage bulb was normally capped with a vacuum stopcock (I) to permit convenient

connection to the vacuum manifold for degassing of the mercury. The reference and cathode compartments were connected with a 1 mm capillary tube (K), permitting electrical contact without excessive circulation of the solution. Contact was made with the mercury cathode through a tungsten wire sealed through the glass at Q.

The anode compartment consisted of a glass tube containing a platinum disk and wire spot welded to a tungsten wire sealed through the glass at R. A hole was provided at S to permit transfer of solution through the reference compartment from the mixing compartment, and another near the bottom of the compartment to assist in equilibration of solution levels. The end of the anode compartment was a 3 cm fine fritted-glass disc, permitting electrical contact without appreciable diffusion of radical anions from cathode to anode. The tubing enclosing the fritted glass was ground to a taper joint which fitted the built-up section of the casing, as shown in Figure 2. This inhibited the diffusion of radicals from the cathode compartment to the anode. Various sample holders (0) could be attached at T, evacuated, then receive a small sample of the radical solution generated and be sealed off under vacuum, with the sample frozen in liquid nitrogen.

For a typical run, the compound to be reduced and the supporting electrolyte were weighed into the mixing chamber in amounts sufficient to make 25 ml of a solution about 10^{-3} molar in the hydrocarbon and 0.1 molar in the electrolyte. The apparatus was assembled, greasing joints with Apiezon N and capping the mercury storage bulb with stop-

cock I. The mercury storage bulb was then loaded with triple-distilled mercury (Masero Laboratories) and connected to the vacuum line for about one hour for degassing. With the mercury storage bulb stopcock closed, the system was then connected to the vacuum line at A and pumped for 2-3 hours, warming the electrolyte and flaming out accessible portions of the apparatus to drive off H_2O. After an hour or two had elapsed, bubbles often appeared near the bottom of the mercury storage bulb, and were not easily dislodged; at this point the needle valve was usually opened enough to allow the bubbles (and a small amount of mercury) to escape into the cathode compartment, while pumping on the system. Ultimate vacuum in the system was estimated to be less than one micron Hg by checking for discharge with a Tesla coil and monitoring system pressure with a Consolidated Vacuum Corporation thermocouple vacuum gauge.

With the cell evacuated, the mixing chamber was chilled in liquid nitrogen and about 25 ml of solvent allowed to distill in from the solvent storage bulb. At least 25 ml was required for proper filling of the cell; the amount distilled could be estimated only roughly while frozen, due to the contraction of frozen THF, but the mixing chamber was calibrated so that the final amount of solvent could be determined within 1 ml. With the solvent still frozen, the system was once more connected to the vacuum line to pump out any leakage.

Needle valve B was then closed and the cell disconnected from the vacuum line. The solvent was warmed to room temperature by careful

application of a beaker of alcohol or H_2O, and stirred with the magnetic stirrer until all electrolyte appeared to be dissolved. The solution was then transferred into the anode and cathode compartments by careful tipping, and enough mercury released to make contact with tungsten wire Q and ensure contact of the solution with the fritted glass. Some tipping and manipulation of the cell was required during this process to prevent bubbles from becoming trapped against the fritted glass, thereby reducing electrical contact and electrolysis current. (To minimize this difficulty, the capillary tube should enter the cathode compartment as near as possible to the level of the bottom of the fritted glass.) Once the solution levels in the various compartments had equilibrated, the cell was usually reconnected to the vacuum line at U so that the sample holder and adjacent tubing could be re-evacuated and flamed out during the progress of the electrolysis.

A DC power supply (Ambitrol Transistorized Power Supply Model 4005; 0-40 v., 0-500 ma.), "Triplet" Model 630 ammeter and Hewlett-Packard 410B vacuum-tube voltmeter were connected with the appropriate wiring to E, R and Q so that the maximum voltage between the mercury pool cathode and the reference electrode could be monitored and manually controlled, and the electrolysis current observed.[5] Electrolysis was carried out at a potential just above the first polaro-

[5] Fraenkel, et al. have used a regulated power supply for this purpose, doubtless obtaining better control; see [44] .

graphic half-wave potential (-2.3 V vs. $Ag|AgClO_4$ for anthracene) [118] giving an initial current of 4-5 ma. Fairly complete reduction was generally obtained by maintaining this potential until the current had fallen below one ma, and remained there for several minutes. In the case of terephthalonitrile, best results were obtained by brief electrolysis at the second reduction potential after "complete" reduction at the first potential, as noted in section five.

Alkali Metal Reductions

For metal reductions, sample holders similar to that shown in Figure 3 were prepared from clean, dry tubing. Sidearm B was usually sealed with a thin glass bubble so that the sample holder could be tested for leaks on the vacuum line; testing completed, the bubble was broken off and the sample holder rinsed thoroughly with distilled water and oven-dried before the constriction at D was introduced. Sidearm C was included only when it was desired to examine a radical with and without electrolytes or other substances added to the same sample.

In operation, about two micro-moles of the substance to be reduced were weighed into a small glass cup on a Mettler Type H16 balance. The cups, 6 mm in diameter, were blown from clean 4 mm OD glass tubing, washed and dried, so that they could be dropped directly into the sample holder, facilitating the handling of small quantities of fluffy substances such as anthracene. A corkborer was used to cut a small pellet of sodium from the freshly-cut surface of a block of metal which had been washed in benzene and dried; the pellet could then be expelled

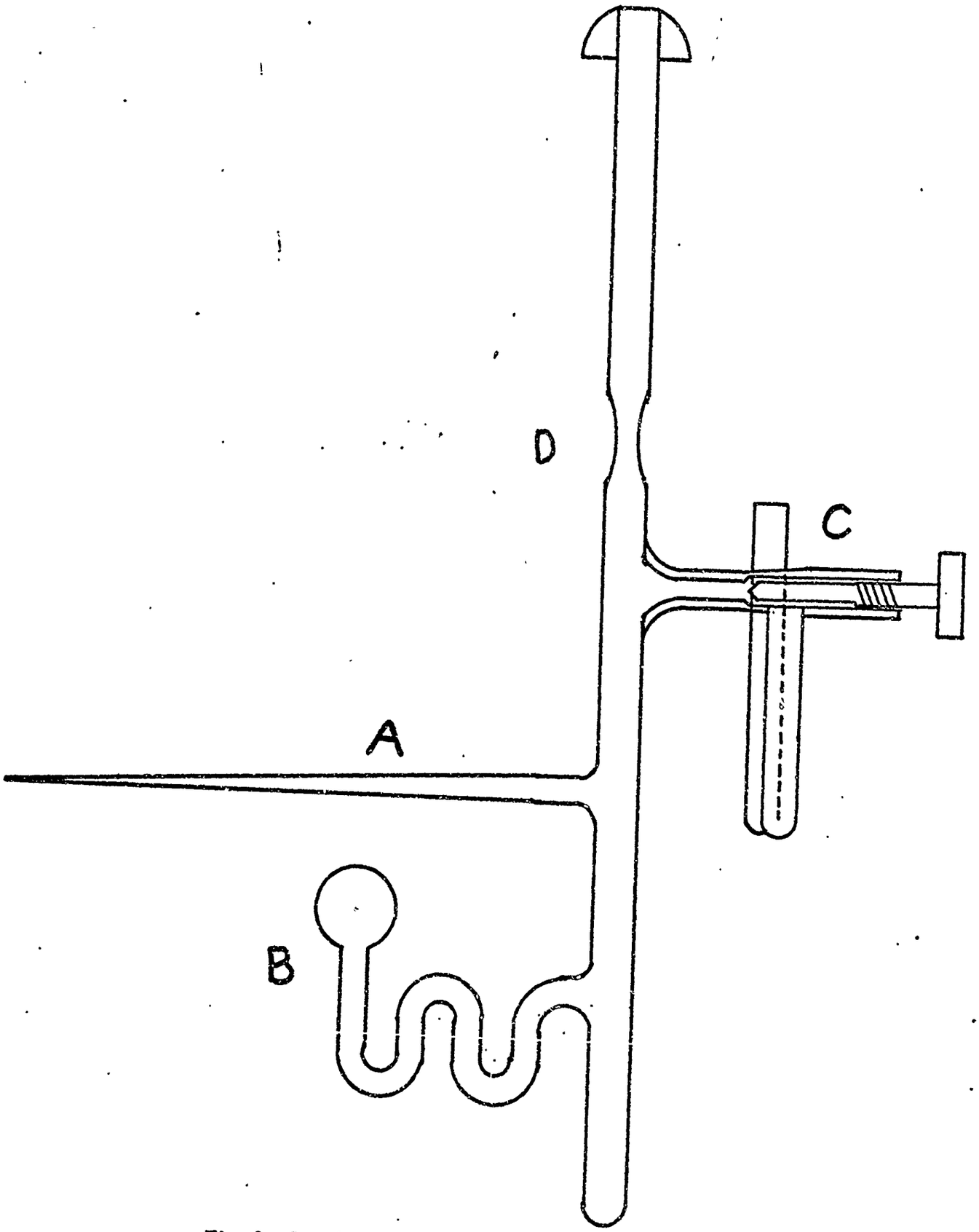

Fig. 3. Sample Holder.

from the cutter directly into sidearm B. The end of the sidearm was sealed off and the sample holder immediately connected to the vacuum line. As soon as the pressure had decreased to about one micron, the sodium was slowly heated in the sidearm to drive off any water or other substances which might have been adsorbed on the metal surface. A thermocouple vacuum gauge (Consolidated Vacuum Corp. GTC-100) was attached to the system so that small changes in pressure could be observed; when more heating ceased to drive off measurable quantities of gas, the sodium was heated more strongly until it just melted, and then was allowed to cool. After repeating this process once or twice, the sodium was considered to be free of volatile impurities, and was vaporized to form a mirror on the wall of the sample holder. Once a satisfactory mirror was formed, sidearm B was sealed off under vacuum and removed. A brown color usually formed on the glass in the sidearm after the sodium had been heated, but appeared to cause nc difficulties, as the sodium vapor could usually be driven over into the sample holder and the sidearm sealed off before the brown coloration had reached the sample holder.

As noted by Bolton and Fraenkel [118] , if the substance to be reduced is at all volatile, it should be protected by immersing the tip of the sample holder in liquid nitrogen once the tube has been evacuated; however, it was found that this procedure tended to allow sodium to condense inconveniently near the bottom of the tube, making it more difficult to control the reduction process. In this work, the samples

were generally not frozen, since the substances examined had relatively low vapor pressures. Even so, vivid colors (often blue, red, or purple) usually formed on the surface of the glass near the mirror, presumably from the reaction of sodium with hydrocarbon absorbed on the glass, and the samples at the bottom of the sample holder were often discolored by similar reactions.

The mirror formed, about two ml of solvent (THF) was distilled in under vacuum, freezing the bottom of the sample holder in liquid nitrogen, and the sample holder sealed off at the constriction while pumping on the system. Interesting color patterns often appeared, as described later. Once warmed to room temperature, the amount of solvent was estimated to 0.1 ml by measuring its height in the tube and comparing with the volume of a similar measuring tube. When several runs were to be made in one day, the samples could be prepared in rapid succession, keeping them frozen in liquid nitrogen until it was time to examine their EPR spectra. With the sodium concentrated near the top of the sample holder and the solution at the bottom, the sample holder could be tipped carefully to allow controlled reduction of the sample, important since most of the substances studied would readily accept a second electron. The resulting solution could be tipped into capillary sidearm A, which was inserted into the Varian all-purpose cavity for EPR observations. Particles of sodium metal were observed in the solutions after the reductions had been carried out; following Ayscough and Wilson [96] , on several occasions the radical solution

was filtered through a ball of glass wool placed in the capillary sidearm. However, the radicals generally decayed on contact with the glass wool, presumably due to adsorbed H_2O (despite heating of the glass wool while the sample holder was evacuated), and this nicety was omitted. Since concentration and degree of reaction are both critical in the observation of well-resolved, intense spectra, the solution was often reacted with the sodium and re-observed several times to determine the optimum signal and to examine the ultimate reduction products (usually diamagnetic).

Concentration could be conveniently controlled by tipping a small amount of radical solution into sidearm A, then chilling the sidearm in liquid nitrogen and distilling in pure solvent to set up a concentration gradient, as suggested by Bolton and Fraenkel [118] . Sidearm A was attached to the tube at a slight angle, so that any radical solution which was not contained in the capillary when the sample was placed in the spectrometer would remain near the bottom of the tube, safely out of reach of the sodium.

Sidearm C, as previously mentioned, was used when it was desired to add an electrolyte (usually TBAP) once the radical solution itself had been observed. The electrolyte was weighed and deposited in the U-tube, which was then sealed off at the end. To ensure that no H_2O, etc., were introduced by the elctrolyte, sidearm B was left sealed and the sample holder placed on the vacuum line for 1-2 hours, warming the electrolyte occasionally. The Teflon needle valve could then be

closed, keeping the electrolyte sample under vacuum while the sample holder was removed from vacuum line, the bubble on sidearm B broken, and the radical solution prepared as above. Once the radical solution had been studied, the valve could be opened and the solution tipped into sidearm C to dissolve the electrolyte, then drained back into the tube for study. The valves appeared to provide an excellent seal at the beveled seat, but some leakage past the O-ring could often be detected after several hours. Small amounts of electrolyte could also be introduced directly with the material to be reduced, using a "standard" sample holder.

3. Theory

The Spin Hamiltonian

The effective Hamiltonian describing an unpaired electron in a molecule interacting with a nucleus of non-zero spin in the presence of a magnetic field H may be written, following Rempel [5] , as

$$\mathcal{H} = \vec{H}.\overline{\overline{g}}.\vec{S}. + \vec{I}.\overline{\overline{A}}.\vec{S}. + \left[\frac{\vec{\mu}_e \cdot \vec{\mu}_n}{r^3} - \frac{3(\vec{\mu}_e \cdot \vec{r})(\vec{\mu}_n \cdot \vec{r})}{r^5}\right] , \qquad (3\text{-}1)$$

where

$\beta = eh/4\pi mc$ is the Bohr magneton,

$\vec{H}$ is the applied magnetic field,

$\vec{S}$ is the electron spin,

$\vec{I}$ the nuclear spin,

$\overline{\overline{A}}$ the hyperfine coupling tensor,

$\overline{\overline{g}}$ the spectroscopic splitting tensor,

$\vec{\mu}_e = -g\beta\vec{S}$, the electron magnetic moment,

$\vec{\mu}_n = g_N \beta_N \vec{I}$, the nuclear magnetic moment,

and $\vec{r}$ the vector from the electron to the nucleus.

The first term is the Zeeman interaction of the electron with the magnetic field. Having "spin" and mass, an electron possesses spin angular momentum, $\vec{J}$, and will precess like a gyroscope if a torque is applied. This interaction may be considered classically as follows: [13]

$$\vec{L} = \frac{d\vec{J}}{dt} = \vec{\omega} X \vec{J} \qquad (3\text{-}2)$$

ω is the angular velocity at which the electron's magnetic moment $\vec{\mu}$ precesses because of the applied torque $\vec{L}$, which arises from

$$\vec{L} = \vec{\mu} \times \vec{H} = -\vec{H} \times \vec{\mu} \quad . \quad (3\text{-}3)$$

It may be shown that for a spinning charged particle, $\vec{\mu} = \gamma \vec{J} = \gamma n \vec{I}$, where $\gamma = \vec{\mu} / \vec{J}$ is a scalar called the "gyromagnetic ratio". Substituting, and equating (3-2) and (3-3) to eliminate J,

$$\frac{d\vec{\mu}}{dt} = \vec{\mu} \times (\gamma \vec{H}). \quad (3\text{-}4)$$

Equation (3-4) shows that the vector $\vec{\mu}$ is precessing about $\vec{H}$, for $\vec{H}$ either constant or time dependent. Following Slichter [113], a solution for $\vec{\mu}$ may be obtained by first transforming (3-4) to a coordinate system which rotates at an arbitrary angular velocity $\vec{\Omega}$, giving an equation of motion,

$$\frac{d\vec{\mu}}{dt} = \vec{\mu} \times (\gamma \vec{H} + \vec{\Omega}), \quad (3\text{-}5)$$

which is identical to that for the laboratory system, (3-4), provided the actual field H is replaced by an effective field, $\vec{H}_e = \vec{H} + \vec{\Omega}/\gamma$.

Solution for the motion of $\vec{\mu}$ in a static field $\vec{H} = \hat{k}H_o$ reveals that $\vec{\mu}$ rotates at an angular velocity $\vec{\Omega} = -\gamma H_o \hat{k}$ with respect to the laboratory, where γH_o, called the "Larmor precessional frequency", is identical with the angular frequency at which quantum theory predicts magnetic resonance absorptions will occur.

Slichter demonstrates that for the same field $\vec{H} = \hat{k}H_o$, solution for the eigenvalues of the simple Hamiltonian,

$$\mathcal{H} = -\gamma\hbar H_o I_z \tag{3-6}$$

yields the allowed energies

$$E = -\gamma\hbar H_o m, \quad m = I, I-1, \ldots, -I. \tag{3-7}$$

If this Hamiltonian is perturbed by an alternating magnetic field (much smaller than H_o) perpendicular to the static field,

$$H_{pert} = -\gamma\hbar H_x^o \cos\omega t, \tag{3-8}$$

transitions between the energy levels are allowed for $\Delta m = \pm 1$, giving

$$\Delta E = \hbar\omega = \gamma\hbar H_o. \tag{3-9}$$

Thus, the absorption frequency is $\omega = \gamma H_o$, the Larmor frequency obtained classically.

Slichter also gives a classical analysis of magnetic resonance absorption, considering the effect of an alternating magnetic field upon a magnetic moment which precesses in a static field.

The second term of the effective spin Hamiltonian is the hyperfine interaction, or Fermi contact term, through which a nucleus of spin I splits each of the unpaired electron's energy levels into 2I + 1 levels. Considering H to be along the z axis, the Hamiltonian is written:

$$\mathcal{H} = g_{zz}\beta HS_z + A_x I_x S_x + A_y I_y S_y + A_z I_z S_z . \tag{3-10}$$

For high fields H, it may usually be assumed that the Zeeman splitting, $g\beta HS_z$, is much greater than the hyperfine splittings A_x, A_y and A_z. Slichter [11] demonstrates that in this case, $\mathcal{H}$

commutes with S_z to a good approximation, and the eigenfunctions may be taken to be eigenfunctions of S_z, with eigenvalues m_S. Thus, $A_z S_z I_z$ is diagonal in m_S, while $A_x S_x I_x$ and $A_y S_y I_y$, having no matrix elements diagonal in m_S, may be dropped in the first order Hamiltonian, giving energy levels

$$E = g\beta Hm_S + AMm_S. \qquad (3\text{-}11)$$

Here, M, the magnetic quantum number of the nucleus, takes values -I, -I+1,...,I, and m_S, the electron spin quantum number, takes values $\pm$ 1/2. $\overline{A}$ and $\overline{g}$ have been spatially averaged to scalars.

Rewriting the energy levels as

$$E = g\beta (H + AM/g\beta)m, \qquad (3\text{-}12)$$

the hyperfine interaction is seen to be equivalent to a local magnetic field AM/g produced at the electron by the nucleus. For a transition between these hyperfine levels, the electron spin "flips", giving $\Delta m = \pm 1$, while the nuclear spin is unchanged. Thus, absorptions occur for fields of $H = h\nu/g\beta \pm A/2g\beta$, separated by $\Delta H = A/g\beta$.

The hyperfine coupling constant A, a measure of the s-character of the electronic wave function at the nucleus in question, is given by

$$A = \frac{8\pi}{3} g_N \beta_N g \beta |\Psi_o|^2, \qquad (3\text{-}13)$$

where Ψ_o is the ground state electronic wave function of the system, and g_N and β_N pertain to the nucleus. [113] Since $|\Psi_o|^2$ is equivalent to the charge density of the unpaired electron at the position of the nucleus, the magnitudes of hyperfine couplings provide experi-

mental data on the spin densities at various nuclei. It will be shown later that this can be extended to a relationship between the hyperfine coupling constants of protons in an aromatic system and the spin densities of an unpaired pi-electron at the carbon atoms of the ring system.

The third term in the spin Hamiltonian is the dipole-dipole interaction between the electronic and nuclear spins, often referred to as the anisotropic hyperfine interaction, and may be written to first order [51] as

$$\mathcal{H} = g\beta\, g_N \beta_N \frac{(3\cos^2\theta - 1)}{r^3} I_z S_z \text{ , where} \qquad (3\text{-}14)$$

θ = the angle between r and the magnetic field H. To be included in the spin Hamiltonian, this term must be averaged over the spatial wave function of the unpaired electron. It may be shown that in a liquid, if a molecule is tumbling rapidly enough, the term $(3\cos^2\theta - 1)$ will average over all solid angles to zero, and splitting of the energy levels due to this interaction will not be observed, although viscosity-dependent broadening or narrowing effects may still arise. [103]

Analysis of Spectra

It has been shown that the hyperfine interaction between an unpaired electron and a nucleus of spin 1/2 (i.e., a hydrogen atom, or "proton") leads to two allowed transitions, separated by an interval equal to the hyperfine coupling constant (usually expressed in gauss). Extending the system to a molecule, say an aromatic hydrocarbon, with an unpaired

electron present, several protons or other magnetic nuclei will interact with the electron's spin, resulting in additional allowed transitions. Those nuclei which are "equivalent" by symmetry (at least on the average) will have the same coupling constant and produce successive splittings of the energy levels when considered in turn. [103] By referring to Figure 4 (a), it may be seen that n equivalent protons lead to n + 1 hyperfine lines, with the overlapping of lines leading to relative intensities which are proportional to the coefficients of a binomial expansion of order n.

For n nuclei with non-zero spins, (2nI + 1) hyperfine lines result; the intensity ratios are most easily considered individually for each case. Some examples are:

One nitrogen (I=1) : three lines, intensities 1:1:1

Two equivalent nitrogens: five lines, intensities 1:2:3:2:1

One sodium (I= 3/2) : four lines, intensities 1:1:1:1

Two equivalent sodiums: seven lines, intensities 1:2:3:4:3:2:1

When two or more non-equivalent sets of nuclei are present, the hyperfine pattern of one set may be considered to be further split by each succeeding set, with the final intensity ratios adjusted accordingly. As shown in Figure 4 (b) with two sets of protons, complex patterns of overlapping or nearly overlapping lines often result when the coupling constants for non-equivalent sets of nuclei happen to be nearly equal.

In Figure 1 (b), the spectrum of the anthracene anion radical has

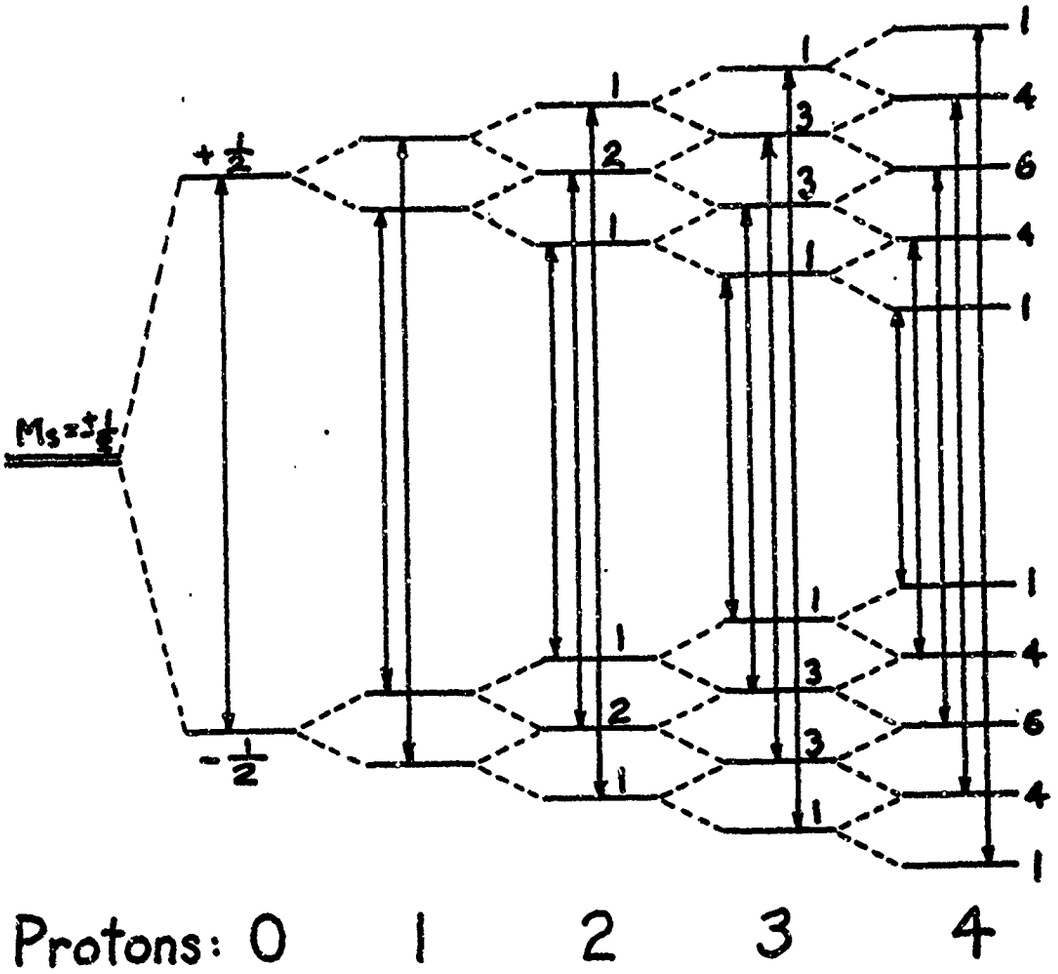

Fig. 4 (a). Hyperfine energy levels resulting from interaction of an unpaired electron with various numbers of equivalent protons. Arrows indicate allowed EPR transitions; numbers refer to degeneracies of energy levels and resulting intensity ratios of transitions. [98]

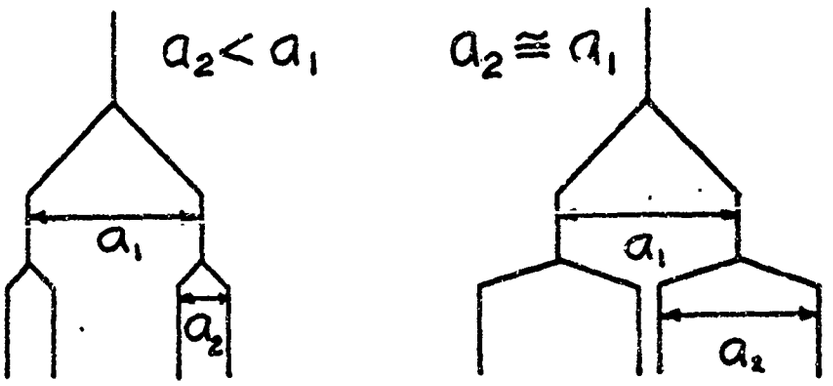

Fig. 4 (b). Hyperfine splittings for two non-equivalent protons.

been reconstructed from the experimental coupling constants; comparing this with the experimental spectrum, Figure 1 (a), (displayed as the derivative of the absorption of microwave power), it may be seen that many lines are too close together to be resolved, and that the lines in the "wings" of the spectrum may not be observed under the same experimental conditions as the far more intense central lines.

Obviously, the analysis of an experimental spectrum will be far more difficult than the reconstruction of a "stick" diagram of line positions and intensity ratios. Generally one can determine ahead of time which sets of nuclei should be equivalent, but the experimental results are occasionally not those expected. Coupling constants are difficult to predict with any accuracy, and slight differences may change the appearance of complex spectra drasticallly. It is often best to observe the wings of the spectrum under conditions which maximize the intensitier of these lines, examine them to obtain coupling constants, and reconstruct the overall spectrum for comparison with experiment. One must still be alert to the possibility of unobserved lines, especially with the intensity ratios of the central portions of two predicted splittings are similar; for instance, the splittings for two equivalent nitrogens (1:2:3:2:1) might easily be confused with those of four equivalent protons (1:4:6:4:1).

Relaxation Effects and the Bloch Equations

Following the discussion by Slichter [13], consider a macroscopic system of nuclei of spin 1/2 in which a resonance is to be observed.

The energy levels are as shown, with the numbers of nuclei in the two m-states + 1/2 and - 1/2 defined as N_+ and N_-, respectively.

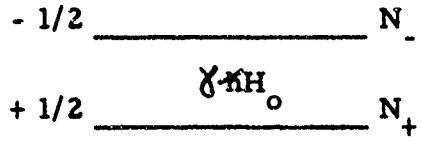

Figure 5. The energy levels for I = 1/2.

The total number of spins, $N = N_+ + N_-$, is constant, but N_+ and N_- will change if transitions are induced by applying an alternating field; by studying the effect of radiation on the population difference, it should be possible to determine the rate of absorption of energy. Define the probability per second of inducing a transition of a spin from a state m = + 1/2 to m = - 1/2 by $W_{+/-}$, and that for the reverse transition as $W_{-/+}$. The differential equation for the change of population N_+ can be written,

$$\frac{dN_+}{dt} = N_- W_{-/+} - N_+ W_{+/-} . \qquad (3\text{-}15)$$

Using time-dependent perturbation theory, Slichter demonstrates that $W_{-/+} = W_{+/-} = W$. It should be noted that in this case, spontaneous transitions from the upper to the lower state, important in optical transitions, are negligible compared with the transition probability due to the rotating magnetic field. [154]

Using the transition probability W and defining the population difference $n = N_+ - N_-$ to eliminate the variables N_+ and N_-, (3-15) may

be written as

$$\frac{dn}{dt} = -2Wn, \tag{3-16}$$

with a solution

$$n = n_o e^{-2Wt}, \tag{3-17}$$

where n_0 is the value of n for t = 0.

Thus, the rate of absorption of energy, dE/dt, may be written as

$$\frac{dE}{dt} = Wh\nu(N_+ - N_-) = Wh\nu n. \tag{3-18}$$

It is apparent that n must be non-zero and negative for a net absorption to occur; but (3-17) implies that any population difference will decay to zero under the influence of induced transitions. For continued resonant absorption, transitions from the upper state to the lower must occur, with the spins giving up energy (as heat) to some other system; the steady state population difference will depend on the willingness of the reservoir to accept energy, i.e., its thermodynamic temperature. Thus, the steady state populations are given by

$$\frac{N_-^o}{N_+^0} = e^{-\Delta E/kT} = e^{-\gamma\hbar H_o/kT} \tag{3-19}$$

Suppose that the spins are coupled to another system (the reservoir), and that this coupling gives rise to a mechanism for inducing transitions between N_+ and N_-; if the probability per second of such a spin transition upward (from + to -) is W_u, and that for the reverse is W_d, it may be

shown [113] that

$$\frac{W_u}{W_d} = \frac{N_-^o}{N_+^o} = e^{\gamma \hbar H_o / kT}. \qquad (3\text{-}20)$$

W_u and W_d are unequal, even though $W_{+/-} = W_{-/+}$, because this thermal transition requires not only a spin coupling, but the existence of another system in a suitable energy state for the transition. To illustrate with a simple case, if the reservoir and nuclear systems each have only two energy levels, with equal spacings, it develops that simultaneous transitions are allowed only for cases in which energy is conserved, as illustrated in Figure 6.

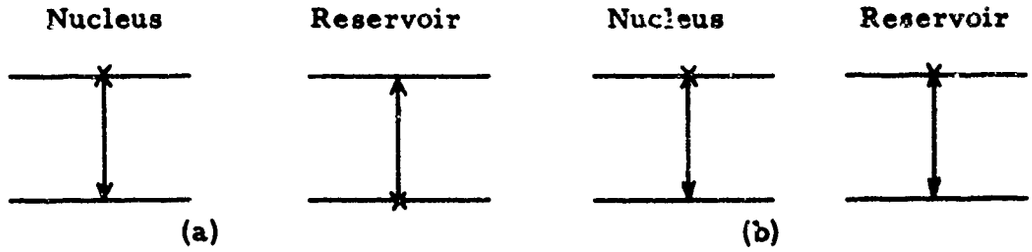

Figure 6. Possible (a) and forbidden (b) spin transitions.

Thus, the rate at which spin transitions occur will depend upon the probability that the reservoir is in an appropriate state as well as upon the matrix elements for the transition.

Defining n_s, the steady state value of n (the population excess in the lower state at thermal equilibrium) as

$$n_s = \frac{W_d - W_u}{W_d + W_u} (N), \qquad (3\text{-}21)$$

and the spin-lattice relaxation time T_1,

$$T_1 = (W_d + W_u)^{-1} , \tag{3-22}$$

the rate equation for n may be written

$$\frac{dn}{dt} = \frac{n_s - n}{T_1} \tag{3-23}$$

The solution of this equation is

$$n = n_s + Ae^{-t/T_1} , \tag{3-24}$$

where the inverse of the time T_1 is the total probability for the occurence of a spin transition through thermal interaction with the reservoir and is called the spin-lattice relaxation time, since the "lattice" (solid, liquid or gas phase) surrounding the nuclei is normally the reservoir involved.

Hameka [54] provides a simple introduction to the Bloch equations, a phenomenological description of the interaction between a system of nuclei of non-zero spin in a homogeneous magnetic field, a rotating perpendicular field, and a thermal reservoir. Since transitions between spin states may be caused by interactions with both the rotating field and the lattice, the rate equation for n becomes

$$\frac{dn}{dt} = -2Wn + \frac{n'_s - n}{T_1} , \tag{3-25}$$

combining (3-16) and (3-23). The solution is

$$n = n''_s + (n_o - n''_s) \exp -t(2W + 1/T_1) \quad , \tag{3-26}$$

where $n''_s = n'_s / (1 + 2WT_1)$ is the steady state value at t = infinity.

The equation of motion of a magnetic moment in a magnetic field, written with respect to a rotating coordinate system, is

$$\frac{d\vec{\mu}}{dt} = \vec{\mu} \times (\vec{\omega} + \gamma \vec{H}) \; ; \tag{3-27}$$

combining this with the equation for the approach of thermal equilibrium by the z component of the total magnetic moment, M_z,

$$\frac{dM_z}{dt} = \frac{M_{z\epsilon} - M_z}{T_1} \quad , \text{ with } M_z = 1/2 \, \hbar \, \gamma \, n \quad , \tag{3-28}$$

the equations of motion for M are

$$\frac{dM_z}{dt} = \frac{M'_z - M_z}{T_1} + \gamma (\vec{M} \times \vec{H})_z \tag{3-29}$$

$$\frac{dM_x}{dt} = \frac{-M_x}{T_2} + \gamma (\vec{M} \times \vec{H})_x$$

$$\frac{dM_y}{dt} = \frac{-M_y}{T_2} + \gamma (\vec{M} \times \vec{H})_y \tag{3-30}$$

Equations (3-30) describe the motion of M_x and M_y; T_2 is the transverse relaxation time, different from T_1 since it is assumed here that only spin-spin relaxation is involved, and $M'_x = M'_y = 0$.

Equations (3-29) and (3-30) are the Bloch equations. For the case of a homogeneous field, H, along the z axis, and a much smaller

rotating field in the x-y plane, $\vec{H}' = H' \cos \omega t$, the equations may be transformed into the rotating coordinate system of $\vec{H}'$ by simply adding $(\vec{\omega} / \gamma)$ to the field $\vec{H}$. The resulting equations yield approximate solutions which may be transformed back to the laboratory coordinate system; replacing M_z' by $\chi_o H$, ω by $-\omega'$ and γH by ω_o,

$$\vec{M} = (M_x + iM_y) e^{-i\omega' t} = \chi \vec{H}' \quad , \tag{3-31}$$

where $\vec{H}' = H' e^{-i\omega' t}$ and the complex susceptibility is $\chi = \chi' + i\chi''$, with

$$\chi' = \frac{(\omega_o - \omega')T_2}{1 + (\omega_o - \omega')^2 T_2^2} \omega_o T_2 \chi_o \quad ,$$

$$\chi'' = \frac{\omega_o T_2 \chi_o}{1 + (\omega_o - \omega')^2 T_2^2} \quad . \tag{3-32}$$

The quantities (3-32) provide a macroscopic description of the magnetic properties of a sample. If the sample is placed in a coil of inductance L_o through which is passed an alternating current of frequency ω', the amount absorbed is proportional to χ'', and will have a maximum for $\omega' = \omega_o$, giving a Lorentzian resonance curve as a function of ω' (Figure 7).

Solutions of the Bloch equations thus describe the position, intensity and shape of magnetic resonance absorption lines; by superposition, the EPR spectrum of a free radical displaying hyperfine structure will be the summation of the χ'' functions for many lines, plotted as a

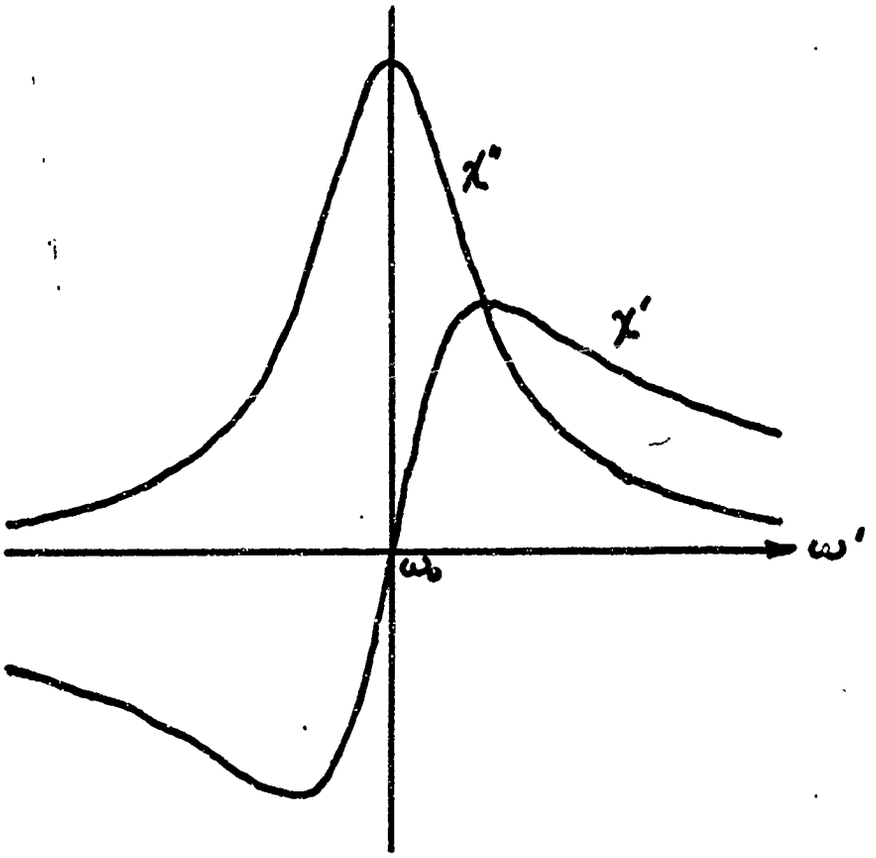

Fig. 7. Absorption (χ'') and dispersion (χ') modes of the Lorentzian line shape function. [14]

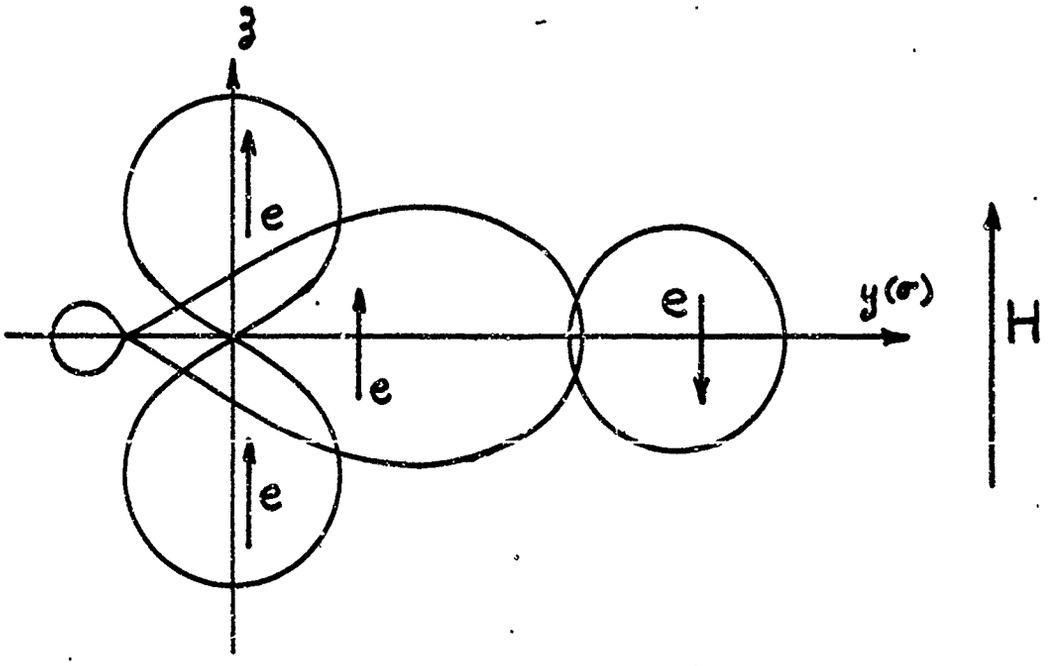

Fig. 8. Electron orbitals in a C-H bond. [115]

function of magnetic field H since ω' is proportional to H. Modified forms of the Bloch equations can be used to describe departures from ideality such as the alternating linewidth phenomenon, discussed later in this section.

Proton Hyperfine Structure and Spin Densities

It was stated earlier that the hyperfine coupling constant for the interaction of a given nucleus with an unpaired electron is a measure of the s-character of the electronic wave function at the nucleus. In the earlier days of EPR, it was not expected that an unpaired electron in the pi orbital of an aromatic free radical would interact with the sigma-bonded ring protons, since the pi orbital has a node in the plane of the ring. The discovery of hyperfine structure apparently due to protons in the EPR spectra of various aromatic hydrocarbons by Lipkin, et al. [6] was therefore quite surprising, and led to a suggestion that the splittings might arise from zero point vibrations of the protons. [7] This was quickly rejected when studies of deuterated radicals [16] showed that the coupling constants were dependent upon the magnetic moment, but not the mass, of the nucleus.

It was subsequently demonstrated by McConnell [19] and Bersohn [15], using valence-bond theory, and Weissman [21], using the molecular approach, that the coupling was due to negative spin densities on the protons, resulting from the mixing of the ground state wave functions with those of excited states involving sigma-pi exchange interactions.

Symons [115] and Carrington [98] have given simple explanations of this phenomenon.

Figure 8 illustrates a $=\dot{C}H$ fragment of an aromatic system, isolated from the rest of the molecule. The positive spin density resulting from the unpaired electron and the bonding electron in the p_z orbital on the carbon will polarize the spin in the sp^2 sigma (y) carbon orbital, this spin polarization also being positive, due to Hund's rule of maximum multiplicity for orthogonal orbitals. The spin on the proton thus tends to be negative, since it must oppose the spin of the other bonding electron, according to the Pauli exclusion principle. Both the negative spin density on the proton[44] and the positive spin density on carbon [36] have been verified experimentally.

Since this spin density on protons is dependent upon a polarization effect, the observed splittings might be expected to be small, and indeed, a proton hyperfine splitting of about 23 gauss is found for a unit unpaired-spin density on the carbon atom (i.e., an unpaired electron localised in a single 2p pi orbital), while the hydrogen atom itself gives a splitting of 500 gauss. In addition, the spin densities at the carbons in aromatic radicals are typically much smaller than unity. Experimental coupling constants are of particular interest because they have been found to vary almost linearly with the spin densities on the carbon atoms considered.

McConnell [29], [30], [31] proposed the relation

$$a_H = Q\rho_C, \qquad (3\text{-}33)$$

where Q, a semi-emprical constant taken to be the same for all C-H bonds, is a negative number, thus giving negative coupling constants for positive spin densities on carbon. Q actually varies with bond angle; thus, a standard value for the absolute value of Q has been the total spread of the EPR spectrum of the benzene anion radical, 22.5 gauss.[5] Since negative or positive couplings lead to the same EPR spectrum, the absolute value of Q is of primary interest to experimentalists. As measured, Q ranges from 20 to 30 gauss for aromatic radicals, generally increasing with the size of the molecule, since larger systems may have several carbons not bonded to protons and negative spin densities may occur at some proton-bonded carbons. McLachlan [46] notes Carrington's experiments with the cation and anion radicals of hydrocarbons [33] which suggest a small variation in Q with the electric charge on the carbon atom, and estimates Q to be 23-24 for a neutral carbon atom, varying within $\pm$ 10% between different positions in the molecule. Since the coupling constants for the cation radicals tend to be greater than those in the anions, with the greatest differences occurring at the positions of high charge density, McLachlan suggests that negative charge may cause the electron cloud of the C-H bond to expand, thus decreasing the hyperfine interaction, while positive charge would have the opposite effect.

Colpa and Bolton [101] have pursued these ideas further, concluding that a better relation between spin density and hyperfine coupling

5. Although this value has been reported by many observers, it has been reported that Q for benzene anion radical is temperature-dependent. [125]

constants is obtained by taking into account the excess charge density on the C-H bond. Their formula is

$$a_H = -(Q + K\epsilon)\rho \quad ; \tag{3-34}$$

using Hückel LCAO-MO calculations of spin densities, $|\epsilon| = \rho$, and the equation may be written

$$a_H = -(Q\rho \pm K\rho^2), \tag{3-35}$$

with the sign of the second term chosen positive for positive ions, negative for negative ions. They obtained a good fit of theoretical to experimental coupling constants for the polyacene series, naphthalene through pentacene, with this equation, using Q = 31.2 and K = 17.

The relations between hyperfine coupling constants and spin densities on magnetic nuclei other than protons have not been so extensively developed, and attempts to relate calculations of spin densities to experimental coupling constants must often involve the extraction of empirical constants from extensive experimental data. Karplus and Fraenkel [56] have developed a quantitative theory for the isotropic electron-nuclear spin interactions of carbon 13 (I=1/2) nuclei in pi-electron radicals, considering the splittings observed in their EPR spectra to arise from sigma-pi interactions between the nucleus and atoms bonded to it, polarizing both 1s and 2s electrons. For an sp^2-hybridized carbon atom bonded to three atoms X_i, the hyperfine coupling constant a_C is given by

$$a_C = (S^C + \sum_{i=1}^{3} Q_{CX_i}{}^C)\rho + \sum_{i=1}^{3} Q_{X_iC}{}^C \rho_i \ , \qquad (3\text{-}36)$$

where ρ and ρ_i are the pi-electron spin densities on atoms C and X_i, respectively. S^C determines the contribution of the 1s electrons, while that of the 2s electrons is described by the Q's, $Q_{BC}{}^A$ being the sigma-pi parameter for the nucleus of atom A resulting from the interaction between the bond BC and the pi-electron spin density on atom B. It is suggested that the method is applicable to "all appropriately bonded elements in the first row of the Periodic Table" [56] , but actual utilization of equation (3-36) above requires either determination of the appropriate exchange integrals or enough experimental data for empirical evaluation of the sigma-pi interaction parameters.

Fraenkel, et al. have estimated some of these parameters for C^{13} and N^{14} in aromatic and aliphatic nitrile anion radicals by comparing molecular orbital calculations [87] of the pi-electron spin densities with experimental EPR spectra. [63] , [112] They propose the following equation for the coupling constant due to the nitrogen of a nitrile group:

$$a_N = (P^N + Q_{NC}{}^{'N})\rho_N + Q_{C}{}^{'N}\rho_{C}{}^{'} \ , \qquad (3\text{-}37)$$

where P^N accounts for all of the 1s polarization and the contribution to the 2s polarization arising from the unshared pair of electrons. The quantities $(P^N + Q_{NC}{}^{'N})$ and $Q_{C}{}^{'N}$ were estimated from a least-squares fit of equation (3-37) to experimental splitting constants

of a series of 11 aromatic nitriles, using both Hückel and McLachlan calculations. The results are:

	Hückel	McLachlan
$(P^N + Q_{NC'}{}^N)$ =	$\pm$ (29.7 $\pm$ 4.2) G	$\pm$ (23.1 $\pm$ 1.4) G
$Q_{C'N}{}^N$ =	$\mp$ (13.3 $\pm$ 5.6) G	$\mp$ (6.8 $\pm$ 2.2) G

Fraenkel, et al. suggest that the upper signs are most likely to be correct. If the variation in spin density on the nitrile carbon from one compound to another is neglected, the splitting from the nitrile nitrogen can be considered to be approximately proportional to the spin density on the nitrogen alone:

$$a_N \cong K \rho_N \tag{3-38}$$

The same least-squares fit used for equation (3-37) gives K = 19.8 $\pm$ 0.7 G for Hückel spin densities, and 18.9 $\pm$ 0.4 G for McLachlan calculations.

Thus far the terms "charge density" and "unpaired electron density" have been used interchangeably with "spin density"; however, it should be noted that the actual spin density at a carbon atom is calculated by adding the spins of all electrons at that atom. An excess of α- over β- spins defines a positive spin density, while an excess of β-spins gives a negative density. Carrington [98] gives a short discussion of these phenomena and cites some experimental evidence of negative spin densities at carbon atoms. Simple Hückel molecular orbital theory predicts only positive electron densities, ranging from

zero to one, and thus may be expected to fail in predicting the EPR spectra of certain radicals; it turns out that self-consistent field theory (involving the mixing of the ground state wave function with those for appropriate excited states) does a better job, often predicting negative spin densities for positions at which the Hückel densities are very small or zero. [46]

Molecular Orbital Theory

Molecular orbital theory has already been mentioned more than once in this paper; although well-discussed elsewhere [65] , [55] , it will also be briefly introduced here, following Streitweiser closely. To calculate the energies (and other interesting quantities) of the electrons in unsaturated organic compounds with meaningful accuracy and a reasonable minimum of labor requires many astute assumptions and approximations. Assuming that the energies of the nuclei, sigma and pi electrons can be separated, the wave function for all pi electrons, ϕ_π , is taken to be aproduct of two-electron molecular orbitals, each being a linear combination of $2p_z$ atomic orbitals (LCAO-MO). The total energy of electrons in the pi-system is given by solutions of the Schrödinger equation, $H_\pi \phi_\pi = E_\pi \phi_\pi$. The molecular orbitals, of the form

$$\psi_j = C_{j1}\phi_1 + C_{j2}\phi_2 + \ldots + C_{jn}\phi_n + \sum_{r=i}^{n} C_{jr}\phi_r \ , \qquad (3\text{-}39)$$

are eigenfunctions of the Hamiltonian operator for the pi-electrons alone. The coefficients C are to be chosen using the variation principle,

which states that

$$E = \frac{\int \psi_H \psi \, d\tau}{\int \psi^2 d\tau} \geq E_o \,, \tag{3-40}$$

i.e., any wave function chosen for the system other than the correct one will lead to a ground state energy E which is higher than the true value E_o. Thus, the best set of coefficients will be that which yields the lowest value of E in equation (3-40), and may be found by minimizing E with respect to each of the coefficients, using $\partial E / \partial c_r = 0$.

If (3-39) is substituted in (3-40), and E minimized with respect to each of the n c_r's, a system of n equations results:

$$\begin{aligned} &c_1 (H_{11}-S_{11}E) + c_2(H_{12}-S_{12}E) + \ldots + c_n (H_{1n}-S_{1n}E) = 0 \\ &c_1(H_{21}-S_{21}E) + \ldots\ldots\ldots\ldots\ldots + c_n (H_{2n}-S_{2n}E) = 0 \\ &\ldots\ldots\ldots\ldots\ldots\ldots\ldots\ldots\ldots\ldots\ldots\ldots\ldots\ldots \\ &c_1 (H_{n1}-S_{n1}E) + c_2(H_{n2}-S_{n2}E) + \ldots + c_n (H_{nn}-S_{nn}E) = 0 \end{aligned} \tag{3-41}$$

Here,

$$H_{rs} = \int \bar{\psi}_r H \bar{\psi}_s \, d\tau = H_{sr}, \text{ and } S_{rs} = \int \phi_r \phi_s \, d\tau = S_{sr}. \tag{3-42}$$

The terms H_{rr} are the Coulomb integrals, representing the approximate energy of an electron in a 2p-orbital. For the pi-lattice of an aromatic hydrocarbon all H_{rr} will be assumed equal, and replaced by the symbol α. The resonance or bond integrals are given by the terms H_{rs} $(r \neq s)$, and represent the energy of interaction of two

atomic orbitals. Since this interaction energy will depend upon the distance between the two orbitals, or bond length, it will be assumed that $H_{rs} = 0$ for unbonded atoms r and s, but for planar molecules with equal bond lengths throughout, $H_{rs} = \beta$ for all bonded atoms. (Note that α and β are negative energy quantities relative to E = 0 for an electron at infinity.)

The overlap integrals S_{rs} are assumed to vanish for $r \neq s$ in the simplest approach, and $S_{rr} = 1$ for normalized atomic orbitals. With these definitions, the system of equations (3-42) becomes

$$\begin{aligned} c_1(\alpha - E) + c_2\beta_{12} + \ldots + c_n\beta_{1n} &= 0 \\ c_1\beta_{21} + c_2(\alpha - E) + \ldots + c_n\beta_{2n} &= 0 \\ \ldots\ldots\ldots\ldots\ldots\ldots\ldots\ldots\ldots\ldots\ldots\ldots & \\ c_1\beta_{n1} + \ldots\ldots\ldots\ldots + c_n(\alpha - E) &= 0 \ , \end{aligned} \qquad (3\text{-}43)$$

with $\beta_{rs} = \beta_{sr} = \beta$ or 0, depending upon whether atoms r and s are considered bonded or non-bonded, respectively. A nontrivial solution is obtained for this system of equations if the secular determinant vanishes:

$$\begin{vmatrix} \alpha - E & \beta_{12} & \beta_{13} \cdots & \beta_{1n} \\ \beta_{21} & \alpha - E & \beta_{23} \cdots & \beta_{2n} \\ & \ldots\ldots\ldots\ldots\ldots\ldots & & \\ \beta_{n1} & \ldots\ldots\ldots\ldots\ldots\ldots & \alpha - E & \end{vmatrix} = 0 \qquad (3\text{-}44)$$

Expansion of this determinant yields the characteristic equation, with n real roots of the form

$$(\alpha - E) = -m_j\beta \quad , j = 1, \ldots, n; \text{ or, } E_j = \alpha + m_j\beta.$$

The positive m_j's represent energy levels which are lower, thus more stable, than the energy of an electron in a single carbon 2p-orbital; these levels are called bonding levels, corresponding to bonding molecular orbitals, while the orbitals for negative m_j are antibonding. For $m_j = 0$, the orbital is described as nonbonding, since its energy is the same as that of an electron in a single carbon p-orbital.

The n energy values thus obtained may be substituted individually into (3-43), giving n sets of n simultaneous equations which may be solved for values of all the coefficients, provided the normalization condition is applied so that $\sum_r c_r^2 = 1$. It can be shown that c_r^2 represents the probability that an electron in a given molecular orbital is to be found in the region of space associated with the atomic orbital r; thus, the total "electron density" at an atom, ρ_r, is the sum of the electron densities contributed by each electron in each molecular orbital:

$$\rho_r = \sum_j n_j c_{jr}^2 \qquad (3\text{-}45)$$

Butadiene, $CH_2{=}CH{-}CH{=}CH_2$, will be considered as a simple example. Using $a = (\alpha - E)/\beta$, the secular determinant becomes

$$\begin{vmatrix} a & 1 & 0 & 0 \\ 1 & a & 1 & 0 \\ 0 & 1 & a & 1 \\ 0 & 0 & 1 & a \end{vmatrix} = 0 . \qquad (3\text{-}46)$$

Solution for the energy levels gives the values shown in Figure 9.

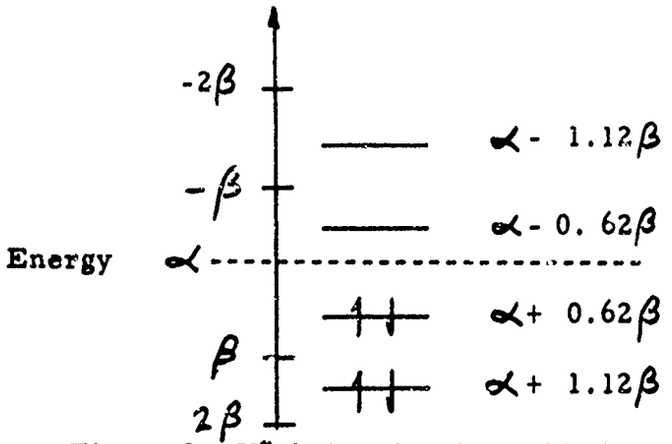

Figure 9. Hückel molecular orbital pi-energy level diagram for butadiene.

The four pi-electrons of the molecule are placed in levels 1 and 2, with spins paired, giving $E = 4\alpha + 4.48\beta$. An extra electron added to butadiene should go in level E_3, the lowest antibonding orbital. For such a radical anion, as for the cation obtained by removing an electron, the charge densities (densities of the unpaired electron) are given by the c_r^2 values for the orbital in which the unpaired electron is accomodated. It is interesting to note that for "alternant" hydrocarbons the pi-electron energy levels are symmetrical about α , i.e., for every bonding orbital with energy $\alpha + m\beta$, there exists an antibonding orbital of energy $\alpha - m\beta$.

An aromatic hydrocarbon is termed "alternant" if one can "star" or label, some of the carbon atoms in such an order that each starred atom is bonded only to unstarred atoms, and vice versa. The terms ever and odd refer to the number of conjugated carbon atoms in the system; in Figure 10, naphthalene (a) is even-alternant, benzyl radical (b) odd-alternant, and azulene (c) non-alternant. The energy

levels of even and odd-alternant hydrocarbons are symmetrical about the α level, but differ in that the odd-alternant molecules have one or more nonbonding orbitals of energy α.

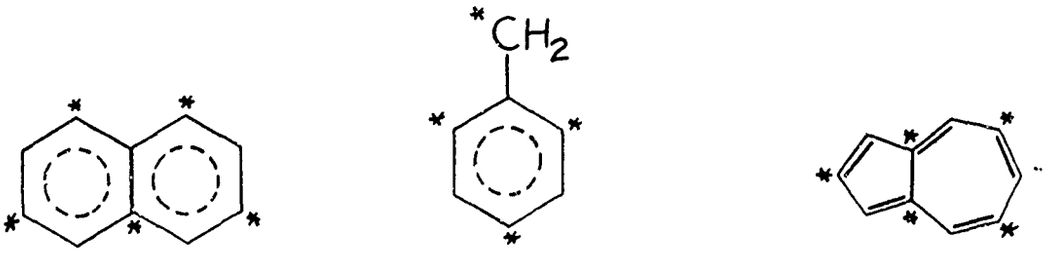

(a) Napthalene (b) Benzyl (c) Azulene

Figure 10. Alternant and non-alternant hydrocarbons

The coefficients of any such pair of molecular orbitals have the same magnitudes; thus the electron densities at corresponding positions are equal, and it is expected (and found experimentally) that the EPR spectra of the radical cations and anions of even-alternant hydrocarbons are very similar.

For any but the most trivial of molecular orbital calculations, the labor is greatly reduced by the application of matrix algebra and numerical solutions by high-speed computers. Assuming some knowledge of matrices, it may be seen that the array of the coefficients of the secular equations (3-43) form the secular matrix, from which the secular determinant is obtained. For simple molecular orbital calculations, the secular matrix will always be a square matrix which is real and symmetric, i.e., the number of rows equals the number of columns, all elements are non-imaginary, and interchanging rows with columns (forming the transpose) leaves the matrix numerically unchanged.

The adjoint $\underline{A}^{\dagger}$ of a matrix $\underline{A}$ is formed by taking the complex conjugate of each element of the transpose, $\underline{A}'$; $\underline{A}^{\dagger} = \underline{A}'^{*}$. For a Hermitian matrix (including real symmetric matrices), the adjoint is the same as the original matrix. A unitary matrix is defined by the fact that its adjoint is also its inverse. A matrix $\underline{A}$ can be transformed to a matrix $\underline{B}$ by a similarity transofrmation with matrix $\underline{C}$: $\underline{CAC}^{-1} = \underline{B}$.

These definitions have application to the matrix equation $(\underline{H} - \lambda\underline{E})$ $x = 0$, where $(\underline{H} - \lambda\underline{E})$ is the secular matrix (3-43), the scalars are eigenvalues of $\underline{H}$, $\underline{E}$ is the unit matrix, and the eigenvectors x are the coefficients of the atomic orbitals within each molecular orbital. The secular matrix, being Hermitian, can be converted to diagonal form by a similarity transformation with a unitary matrix without changing its eigenvalues. Normally, the secular matrix (3-46), with the α's omitted, is transformed by a unitary transformation with the matrix of the molecular orbital coefficients to a diagonal matrix containing the eigenvalues along the diagonal. Jacobi's iterative diagonalization process is often used in computer molecular orbital calculations; this method involves setting up unitary matrices which reduce symmetrical pairs of off-diagonal elements to zero through similarity transformations. By starting with the largest elements first and progressively eliminating all off-diagonal elements, the matrix is diagonalized, giving the eigenvalues, and the product of the transforming matrices converges to the matrix of the eigenvectors, the molecular orbital coefficients.

The importance of molecular orbital theory in making quantitative and qualitative predictions of electron distributions may be illustrated

by considering the molecular orbitals for benzene and some of its derivatives. [98] , [115] Hückel molecular orbital theory combines the six pi-orbitals of benzene into the six molecular orbitals shown in Figure 11, three being bonding orbitals and three antibonding. The squares of the coefficients of the molecular orbitals are included at the appropriate points in the diagram, and the nodes indicated by dotted lines. From the relative energy levels for the orbitals, it may be seen that the highest-energy bonding and lowest-energy antibonding orbitals occur in degenerate pairs. Thus, in the benzene anion radical, the unpaired electron should be distributed equally between the two degenerate antibonding orbitals, giving an average electron density at all carbons of 1/6.

The predicted seven-line EPR spectrum (intensities 1:6:15:20:15:6:1) with spacing Q/6 is matched closely by experimental results [25] (a_H = 3.75 G), except that the individual lines are broader than expected for such an anion radical. This broadening of lines has been explained in terms of spin-orbit coupling [41] , [61] , and will be considered later.

In substituted benzene anions with lower than three-fold symmetry, these orbitally degenerate levels are split; if the perturbation due to the substituent is not too large, the distribution of the unpaired electron will tend to conform to that in either the symmetric or antisymmetric anti-bonding orbital. Considering the perturbation by the substituent(s) (r) as purely an inductive effect, an electron-repelling substituent would cause the unpaired electron to occupy the antisymmetric orbital

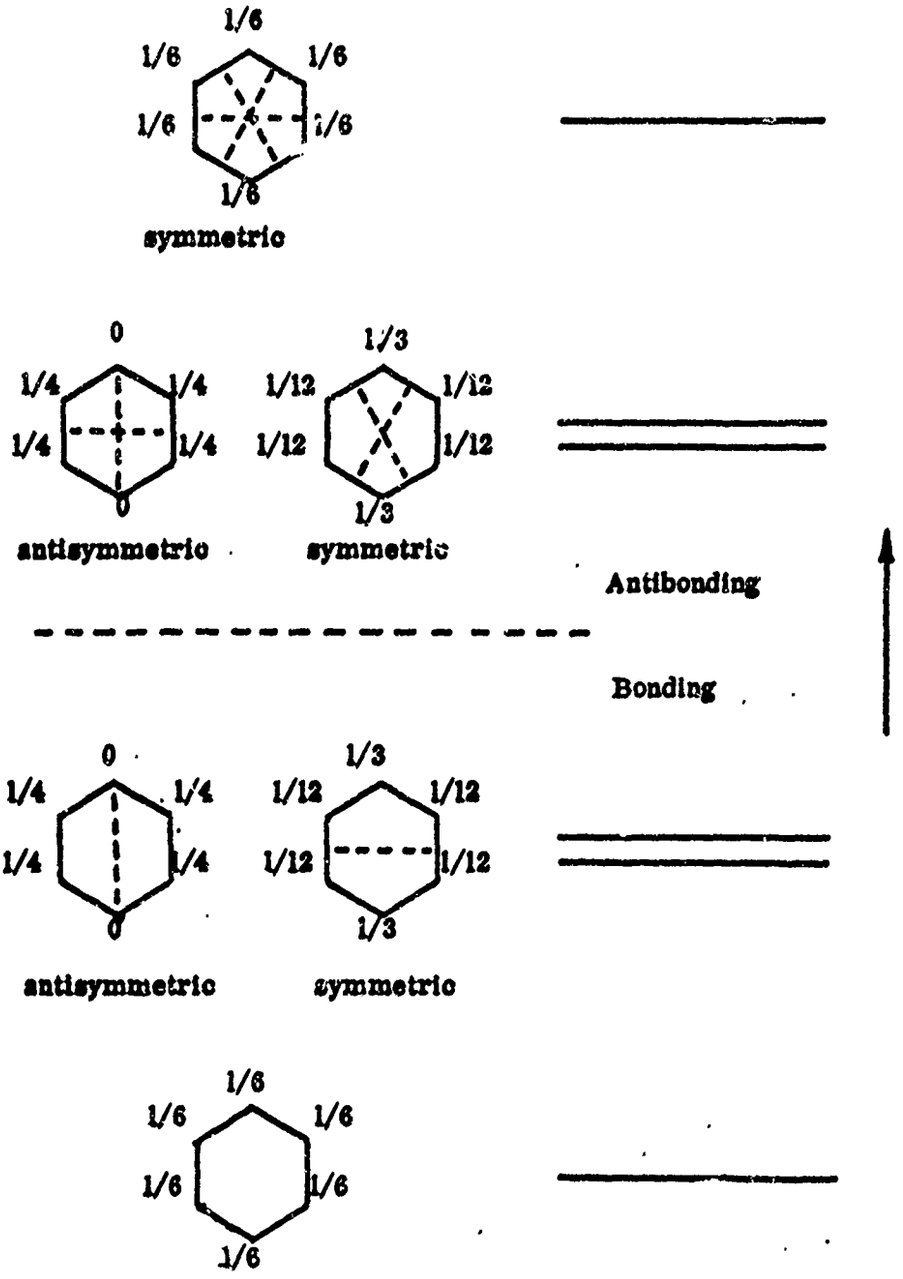

Fig. 11. Molecular orbitals for benzene, with squares of the coefficients indicated. [98] , [115]

(thus avoiding the substituent). The predicted EPR spectrum would consist of a quintet from four equivalent protons ortho and meta to the substituent, with spacing about 5.5 gauss; only very small splittings would be expected from the para proton or magnetic nuclei in the substituent.

Conversely, electron-withdrawing substituents should make the unpaired electron "prefer" the symmetric orbital, since this provides the maximum electron density at the substituent position. Monosubstitution should lead to EPR spectra with a large doublet splitting from the para proton, possible large splittings from substituent nuclei, and smaller splittings from the non-equivalent ortho and meta protons. Para-disubstituted benzene anions would display either two triplet splittings or one quintet, plus substituent splittings, depending upon the spins and equivalence or non-equivalence of the substituents.

For meta-disubstituted benzene anions, electron-repelling substituents should make the unpaired electron occupy the symmetric orbital, with minimum electron densities at the substituent positions, while electron-withdrawing substituents would make it seek the distribution provided by the antisymmetric orbital. Similarly, in the ortho-disubstituted anions, electron-withdrawing or electron-repelling substituents should make the unpaired electron prefer the antisymmetric or symmetric orbitals, respectively. Both Carrington [98] and Symons [115] have reviewed experimental work which illustrates these trends.

If there is considerable pi-bonding between the substituent and

ring, this simple qualitative approach may require modifications, especially when splittings from substituent nuclei are to be considered, as in nitro groups, etc. Even here, simple corrections to Hückel calculations permit the prediction of proper trends, if not the numerical duplication of experimental coupling constants.

It is apparent that consideration of electron distributions calculated by molecular orbital theory can be very useful in the prediction of EPR spectra, particularly for substituted or otherwise perturbed species.

Molecular orbital calculations for compounds whose pi-systems contain heteroatoms (atoms other than carbon) are well-discussed by Streitweiser [65]. Heteroatoms are generally included as carbon atoms in the pi-system would be, with appropriate changes being made in Coulomb and bond integrals. For a heteroatom X (substituent or ring component), the appropriate integrals are expressed in terms of the standard integrals for benzene, as illustrated in (3-47):

$$\alpha_X = \alpha_C + h_X \beta_{CC}$$
$$\beta_{CX} = k_{CX} \beta_{CC} \qquad (3\text{-}47)$$

Estimating the values of h and k which are to be used may be difficult if quantitative results are desired; probably the ideal procedure would be to study the correlation between some experimental quantity and a calculated quantity which is dependent upon the h and k parameters. However, parameters have generally been assigned on the basis of educated guesses or theoretical assumptions; due to this, and the fact

that different approaches to molecular orbital calculations (i.e., inclusion or neglect of overlap) require different parameters, it is difficult to choose the proper parameters for a given calculation directly from the literature.

Streitweiser has compiled a table of suggested parameter values for heteroatoms for use with simple HMO calculations [65] (neglecting overlap), assuming that α_X should be proportional to empirical electronegativities and h_X proportional to electronegativity differences (relative to carbon), that h_X should be greater for a heteroatom which contributes two electrons to the pi-system than for the same heteroatom contributing one, and that β is proportional to the overlap integral S. Obviously, such a table can be only a starting point, and the parameters must be varied to obtain optimum correlation for specific cases.

An example of the "fitting" of calculated pi-electron densities to those measured experimentally as hyperfine splittings in EPR spectra is the work of Rieger and Fraenkel [87], who studied a series of aromatic and aliphatic nitrile anion radicals. Using McConnell's equation, $a_H = Q\rho$, to relate the proton hyperfine coupling constants to the electron densities at the adjacent carbon atoms ($Q = -23.7$ G), and more complicated expressions involving semi-empirically derived constants for splittings from nitrile nitrogens and C^{13}, they estimated values for the Coulomb and bond integrals for the nitrile group by fitting calculated electron densities to the experimental. For the terephthalonitrile anion radical, the best parameters obtained were

$h_N = 1.1$, $k_{CN} = 2.0$ and $k_{CC'} = 0.6$; for the entire series of nitriles, more suitable values were $h_N = 1.0$, $k_{CN} = 2.0$ and $k_{CC'} = 0.9$.

Environmental Perturbation of Radical Anions

Aromatic radical anions may exist in solution in many forms; for a qualitative discussion similar to that of Reddoch, the systems can be given initial classifications of free anions, associated cation-anion pairs, or equilibrium mixtures of these species. [149] The equilibrium mixtures may be subdivided into slow and fast categories; an equilibrium is considered "slow" if the mean lifetimes of the two forms present are long compared to the reciprocals of the differences in their hyperfine coupling constants, expressed in frequency units. These systems generally display superimposed EPR spectra for the two species, the relative intensities varying as the ion pairs dissociate with dilution or decreasing temperature. Atherton and Weissman studied such a system, napthalene reduced by sodium in THF, and were able to determine the equilibrium constant and enthalpy of dissociation by careful study of the intensities of the spectra for the two species. [53]

In "fast" equilibria, both forms have lifetimes short compared with the reciprocals of their hyperfine coupling constants, and the proton coupling constants will be given by averages of those of the associated and dissociated forms, weighted in proportion to their concentration. These coupling constants should thus vary as the degree of dissociation is altered by changing concentrations, temperature, etc.

For such a case of rapid exchange, the hyperfine interaction with the cation is expected to average to zero.

It should be noted that this explanation is highly simplified; solvation will play a major part in determining the structure and behavior of the associated species. Gendell, Freed and Fraenkel have analyzed the perturbations of spin density resulting from interactions between solvent molecules and polar substituents or heteroatoms in localized complexes. [80] They point out that a radical with one or more polar sites may exist in a mixed solvent in many different forms, associated or dissociated, depending upon the symmetries of the various solvated species. Fortunately, the observed coupling constant should still be an average for all species in the limit of rapid exchange for all equilibria.

It would be expected that radicals with polar substituents or heteroatoms would have a greater tendency to form ion-pairs with a given cation than would a hydrocarbon radical, due to the more localized negative charge. Hydrocarbons could vary among themselves, depending upon their charge density distribution and polarizability. Polar radicals often exist in very complex equilibria; as an example, sodium benzophenone ketyl has been found to exist in various solvents in equilibrium mixtures of a paramagnetic monomer, paramagnetic dimer and diamagnetic dimer. [129] , [130]

The actual structures of ion-pairs formed by cations and radical ions have been subject to much qualitative discussion, but little

experimental verification of the details. Studies of aromatic hydrocarbon anions suggest that they exist as free ions under favorable conditions, i.e., high solvent dielectric constant, small radius metal cations and low temperatures. [38] The solvation free enthalpy increases with increasing dielectric constant and decreasing radii of the ions; since the dielectric constant has a negative temperature coefficient, the solvation becomes stronger when the temperature decreases. Ionic association increases with increasing cation radius, decreasing dielectric constant and increasing temperature. Aten, et al. [38] suggest that the ions in ion pairs are separated by at least one layer of solvent molecules.

Tetra-alkyl ammonium salts have become widely used in the electrolytic production of radical anions since it was suggested that such bulky cations should be too large to form tight ion-pair complexes; [35] although they have not been observed to cause cation splitting, it has been noted that the proton coupling constants of hydrocarbon anion radicals seem to be more perturbed by these cations than by those of the alkali metals. [149] , [118] Apparently the smaller alkali metal cations are heavily solvated, thus affecting the radicals less than the weakly-solvated bulky cations; Reddoch points out that the absence of hyperfine coupling with the nitrogen of the ammonium ions could be due to rapid association/dissociation, or to rapid exchange of cations between ion pairs and the large excess of electrolyte. Bolton and Fraenkel conclude from their work with anthracene that there is more ion-pair formation in solutions containing TBAP than in those with

alkali cations; whether TBAP actually has a greater tendency to form ion-pairs than alkali metals was not determined, however, since the relative concentrations differed by a factor of 50.

It should be further noted that these conclusions may well be reversed in the case of radical anions containing functional groups which can form tight complexes with the counterions. [118]

For ion-pairs containing polar radicals, the cation has usually been considered to be localized near the polar site or to oscillate between polar sites if more than one is available. For hydrocarbon radicals, the initial choice is usually the region of greatest negative charge density. Calculations have been made to determine the regions of minimum potential energy for a few molecules, including benzophene and anthracene. [59]

Following the discussion of Reddoch [136], consider a radical R^- in solution, with an equilibrium existing between the "free ion" R^- and a complexed species R^-C^+ which is perturbed by some solute (cation or more polar solvent). For such an equilibrium,

$$R^-C^+ \rightleftharpoons R^- + C^+ \quad , \quad K_{eq} = \frac{(R^-)\,(C^+)}{(R^-C^+)} \quad . \qquad (3\text{-}48)$$

For fast equilibrium, the observed coupling constants will be an average over the couplings of all species present, and can be represented by an equation of the type

$$a_i = a_i^o + P\Delta a_i \quad , \qquad (3\text{-}49)$$

where a_i^o are the coupling constants for the "free ion" in solution and $\Delta a_i = a_i^P - a_i^o$ is the shift in the coupling constants which occurs when the radical is subjected to some maximum perturbation. If it can be assumed that the degree of perturbation is proportional to the fraction of the radicals which exist as the complex R^-C^+, then we may write the "perturbation strength", P, as

$$P = \frac{(R^-C^+)}{(R^-C^+) + (R^-)} = \frac{(C^+)}{K_{eq} + (C^+)} . \qquad (3\text{-}50)$$

This relation would permit the plotting of a series of experimentally determined coupling constants against a function of the concentration of the perturbing species, (C^+), provided K_{eq} was known or could be determined. The development of such a simple linear relationship from experimental data would prove very gratifying, as this should permit extrapolation to a point of zero perturbation strength, where the coupling constants for the true free ion could be compared with those obtained from molecular orbital calculations, etc.

A similar treatment for the effect of mixed solvents on coupling constants is given by Gendell, Freed and Fraenkel [80] ; they were able to reproduce the magnitude and direction of proton coupling constant shifts in semiquinones as the dielectric constant of the solvent was changed, by changing the effective electronegativity of the oxygen in their molecular orbital calculations.

The best system yet to appear for relating observed shifts in coupling constants to the degree of perturbation of the spin density of

a radical appears to be Reddoch's empirical correlation diagram. [149] If coupling constants are available for the same radical prepared under a variety of conditions, two sets of data are picked, preferably for two samples whose coupling constants are precisely determined and differ substantially from each other in value. Generally it is convenient to plot the coupling constants for the "least perturbed" case on a vertical scale at the left side of the diagram, the other case being plotted at the right. If the pairs of points for each coupling constants are then joined by straight lines, an attempt may be made to fit the data for all other samples to these lines by plotting all the coupling constants for each sample vertically above a common horizontal coordinate, chosen to minimize the deviations of the coupling constants from their corresponding lines.

Using horizontal position as the only adjustable parameter, Reddoch was able to fit about 35 sets of coupling constants for anthracene, and 20 for azulene, to straight lines; he concluded that the horizontal axis must be a valid measure of increasing perturbation of the free hydrocarbon anions by their environments, particularly the cations present. This system has the advantage of putting data from preparations with different alkali metals, solvents, electrolytes, etc., all on a common scale of perturbations as exhibited by shifts in the observed coupling constants.

Reddoch calculates the effect of a counterion on the proton coupling constants using a method similar to that used by McClelland [59] and

by Hush and Rowlands. [106] Using the Hückel molecular orbital method to calculate the spin densities for the free anion, the perturbation of the cation is represented by the electrostatic field of a unit positive charge located in the proper position. The change in the wave functions and the coupling constants are then calculated by perturbation theory. Since the coupling constants of the true free ion cannot be determined experimentally, a direct comparison of theoretical and experimental coupling constants is not possible; Reddoch suggests comparing the slopes of the lines on the correlation diagram with the calculated relative shifts of each of the coupling constants as the ion is perturbed. In the case of anthracene, the EPR spectra suggest that the protons which are equivalent by symmetry remain equivalent in the ion pairs. Reddoch points out that this "would not be possible unless the motion of the cation, projected on the plane of the aromatic rings, conformed to the symmetry of the anion". [149] He maintains that the dominant part of the perturbation may be found by placing the cation above the center of the plane of the ion. This position is favored energetically also, due to the large negative charge density on carbons 9 or 10 in the anion. Taking the perturbing charge 3.5 Å above the plane (representing a contact ion pair with an alkali ion), Reddoch calculates relative shifts which match the slopes of the experimental plots in sign and approximate magnitude.

In addition to the systematic shifts in coupling constants caused by perturbations of the radical by the solvent-solute complex, certain

anomalous effects due to ion association and solvation have created considerable interest and frustration in the field of EPR. Carrington has reviewed some recent examples of these phenomena. [19]

The solvent dependence of the EPR spectra of pyracene radical anion associated with various alkali metal cations has been studied extensively by de Boer and Mackor. [102], [122], [142] Reduction of pyracene with potassium in DME at -70 deg. C yields a spectrum which

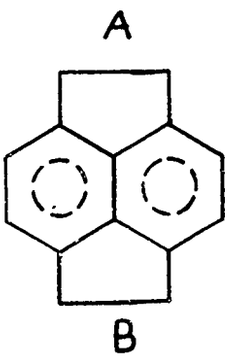

Figure 12. Pyracene

is straightforwardly interpreted as that of the unassociated anion. Reduction with sodium in methyl-THF at -83 deg. C produces a spectrum due to the pyracene $^{-}Na^{+}$ ion pair, in which splitting by sodium is observed and the methylene protons are no longer equivalent, but produce two quintet splittings of slightly different values. Furthermore, reduction with potassium in THF at -30 deg. C yields a spectrum in

which the eight methylene protons are equivalent, but the nine resulting groups of lines display an alternation in line width from the center of the spectrum to the wings. A small potassium splitting is observed.

The line width alternation is interpreted as due to an oscillation of the alkali cation between positions A and B, the two minima in the potential well of the system, which produces a time-dependent modulation of the isotropic coupling constants of the methylene protons. Since the potassium splitting is preserved in the process, the spin orientation of the potassium nucleus must remain unchanged during the transfer, and the rate process may justifiably be considered to be intramolecular. Introduction of an intermolecular cation exchange process by the addition of sodium halides to the sodium-pyracene system resulted in a complete loss of alkali splitting.

In later work with sodium, cesium, rubidium and lithium at lower temperatures [42] , a different line width alternation effect was observed which appeared due to an oscillation of the cation within potential well A or B. The metal coupling constants for rubidium and cesium decreased to zero with changes in temperature, but increased again as the temperature was varied further, leading de Boer to conclude that the spin density at the alkali nucleus is composed of both negative and positive contributions.

Maki and Geske observed the EPR spectrum of para-nitrobenzaldehyde anion, and attributed the non-equivalence of the two protons ortho to the nitro group to a restricted rotation of the aldehyde group

about the C-C bond. [58] Maki reinforced this interpretation by observing an EPR spectrum for terephthalaldehyde anion which corresponded to an equilibrium mixture of the cis and trans forms of the radical. [57] A similar case of conformational interconversion which results in line width alternation has been reported for the anion and cation free radicals of 1, 2, 3, 6, 7, 8-hexahydropyrene. [123]

Bolton, Carrington and Todd have observed line width alternation in the durosemiquinone and naphthazarin semi-quinone cations which they attribute to the hindered rotation of OH groups. [97] , [71] Carrington has analyzed the case of durosemiquinone theoretically, using a modified form of the Bloch equations to derive the shape of the spectrum for different rates of isomerization. [74] Similar line width alternation effects were observed by Fraenkel, et al., [79] , [80] , [81] for the anions of dinitrodurene and meta-dinitrobenzene.

Nitrobenzene anions, particularly the isomeric dinitro species, display some interesting effects of ion pairing. Ward reported that alkali-metal reduction of meta-dinitrobenzene in DME gave a spectrum in which the nitrogens were non-equivalent, one coupling constant being much larger than the other. [52] , [67] Electrolytic reduction in a solvent of high dielectric constant (methyl cyanide) yielded a spectrum showing equal splitting from both nitrogen atoms [43] , while the reduction of meta-dinitrobenzene by potassium in DME, followed by partial removal of the DME and addition of acetonitrile, also produced a spectrum with two equivalent nitrogens. [117] Alternating line widths

have also been observed in the EPR spectrum of para-dinitrobenzene anion in various solvents. [138]

Another example of line width alternation due to intramolecular cation exchange is the recent work reported for the pyrazine $^{-}Na^{+}$ system in THF and/or DME, in which the sodium ion hops from one nitrogen atom to the other, leaving the protons and nitrogens apparently equivalent. [137], [116], [151]

The alternating line width phenomenon seems best described theoretically by the application of relaxation-matrix theory to a general theory of linewidths [103], although, as mentioned earlier, the modified Bloch equations will sometimes suffice. [73] A qualitative discussion can be given following the Freed and Fraenkel treatment of dinitro compounds. [103]

Using their "semiclassical formulation", the total Hamiltonian of a spin system may be divided into two parts,

$$H = H_o + H_1(t) . \qquad (3\text{-}51)$$

H_o, the zero-order Hamiltonian operator, is time independent, giving rise to a sharp-line spectrum, while $H_1(t)$, a fluctuating, time-dependent perturbation causing relaxation and line broadening, is a random function with a time average of zero. $H_1(t)$ includes motions of the radical resulting from collisions with the solvent, internal rotation and vibration and disturbances introduced by complexes formed between the radical and the solvent or other solutes.

Freed and Fraenkel [103] provide some useful definitions of equivalent nuclei, describing two nuclei i and j "equivalent" if the zero-order Hamiltonian is symmetric with respect to their exchange. This implies that $\gamma_i = \gamma_j$, $I_i = I_j$, and $a_i = a_j$; since this may occur not only for nuclei which are located at symmetrically equivalent positions in the molecule, but also for those which simply have the same magnetic properties and hyperfine coupling constants, the two possible cases are described as "symmetrical equivalence" and "accidental equivalence", respectively. (For accidental equivalence, the coupling constants may be considered equal if their difference is much less than the linewidth.)

Nuclei which are equivalent with respect to H_o are not necessarily equivalent with respect to the perturbation $H_1(t)$; therefore, the term "completely equivalent" is used for two nuclei i and j if both H_o and $H_1(t)$ are symmetric with respect to their interchange. Using these definitions, all nuclei in a molecule may be divided into sets of equivalent nuclei, which may be further subdivided into subsets of completely equivalent nuclei. It develops that if a given equivalent set contains more than one completely equivalent subset, alternating line widths and similar phenomena may be observed.

For the "two-jump interchange" case, we consider a radical which can exist in two different states, A and B, which have the same lifetime t; there is an exchange reaction between the two states, with the time of the exchange assumed to be small compared to t. Suppose

further that each nucleus may have only two different splitting constants, a_I or a_{II}, the nuclei exchanging coupling constants as the molecule switches from state A to state B:

$$a_1(A) = a_2(B) = a_I$$
$$a_2(A) = a_1(B) = a_{II} . \qquad (3\text{-}52)$$

Provided the probabilities of occurrence of states A or B are equal, the average coupling constant is the same for each nucleus, and is given by $\bar{a} = 1/2\,(a_I + a_{II})$. For two nitrogens (I=1) with coupling constants a_I and a_{II}, a nine-line spectrum is predicted; in the limit of very long lifetimes for states A and B, one of these coupling constants approaches zero, giving a three line spectrum. As the life-times become very short (rapid exchange), a_I and a_{II} become nearly equal, and the usual five-line spectrum for two equivalent nitrogens is predicted. If the quantum numbers (m_1, m_2) are used to identify the lines of the spectrum, it can be seen that the transition from three lines to five involves shifting all the lines but $(\pm 1, \pm 1)$ and $(0, 0)$. At intermediate exchange rates, the lines for $M = m_1 + m_2 = \pm 1$ are broadened as they shift in position, while lines for $M = \pm 2$ and 0 are left unbroadened. Thus, alternating line width in the case of two equivalent nitrogens reveals itself in narrow central and outer lines, with the two intermediate lines being broader.

Determination of Coupling Constants

The researcher faced with the problem of assigning and measuring precisely the coupling constants of a recorded EPR spectrum will almost certainly rely on the application of rule to paper for the initial assignment phase, but this procedure has serious shortcomings if used for the final determination of coupling values. Even with such equipment as the Varian Fieldial accessory and field sweep, one is advised to calibrate the sweep with standards such as para-benzosemiquinone; an operating NMR gaussmeter-field marker system provides more flexibility and precision, although if the markers are placed at intervals close enough to be convenient, random errors inherent in the measurement and marking process may not be negligible compared with the measurement interval. All these methods are limited by the difficulty of measuring distances to tolerances of less than about .01 inch; the relative error involved could be decreased by using a strip-chart recorder with a high paper speed, but improvement by even an order of magnitude might require one to store recorded spectra like papyrus scrolls or paper walls with them.

If an NMR gaussmeter is available, coupling constants may be determined for well-resolved spectra by choosing several sharp, intense, non-overlapping lines and making repeated measurements of the frequency differences between them. In making these experimental measurements, it is convenient to have a simple but specific designation

for each of the lines involved. Since each line lies at a distance from the spectrum center which is some linear combination of the various coupling constants, a simple vector-style notation was used in this laboratory to denote line positions, treating each coupling constant as a vector component. For a molecule with coupling constants a_1, a_2 and a_3, the line (1 $\bar{1}$ 2) would be located at a distance $(a_1 - a_2 + 2a_3)$ from center. Since each coupling constant may be determined by measurements between several different lines, and these measurements repeated, the average coupling constants may be taken as the "best" values, and the standard deviations calculated for each as a measure of precision.

The determination of the best parameters to fit a complex function such as an EPR spectrum suggests the principle of least squares; the best parameters should be those which minimize the sum of the squared errors when the experimental data is compared with a function computed from said parameters. EPR spectra are calculated in this laboratory by a computer program written in FORTRAN 60 for the Control Data Corporation 1604 digital computer. With binomial coefficients and line spacings inserted for the appropriate sets of equivalent nuclei, the relative intensities and positions of the spectral lines are determined in much the same manner as the preparation of a "stick diagram". A Lorentzian line of the proper intensity and an average linewidth is then "erected" at each position, the lines all summed to give an absorption spectrum, and the more usual derivative form obtained.

The derivative spectrum is scaled to a specified value of the maximum peak-to-peak amplitude, and is then normally plotted by a DRAW subroutine on the CALCOMP 165 X-Y plotter. Spectra may be plotted on paper as large as 9 X 15 inches, the size used for recording experimental spectra. A maximum of 900 points may be plotted on each curve, representing an entire spectrum or small portion thereof as required. Two or more spectra of different species, with the same or differing g values, may be superimposed. Certain second order effects may be introduced by including the proper data.

The least-squares program compares the calculated amplitudes of the envelope of a derivative spectrum (calculated from "best" measured parameters) with a number of such points measured from the central portion of the experimental spectrum, then estimates what should be "better" parameters. Given good initial choices of parameters, a series of iterations permits the program to converge on the parameter values which minimize the sum of the squared errors, or "residual". (Poor initial parameters usually caused the residual to diverge.) Program input data includes the intensity ratios and line spacings for the expected sets of equivalent nuclei ("cases"), measured coupling constants, linewidth, maximum amplitude, number of data points, field spanned by the data (horizontal centering may be accounted for here) and vertical offset. The outputs are the best values of the coupling constants, linewidth, maximum amplitude, horizontal centering and vertical offset; their standard deviations, and the value of the residual.

The least-squares analysis of a function for the best values of several parameters is developed as follows. Given an array of points, z_i, measured from the envelope of the experimental spectrum, a corresponding array f_i may be calculated using the set of parameters, a_j, determined from the experimental spectrum. To refine these parameters, it is desired to minimize the sum of the squared errors between z_i and f_i with respect to each parameter, i.e., to solve the system of equations

$$\frac{\partial}{\partial a_j} \left[\sum_i (z_i - f_i)^2 \right] = 0. \qquad (4\text{-}1)$$

Differentiating,

$$- \sum_i 2(z_i - f_i) \frac{\partial f_i}{\partial a_j} = 0 \; ; \qquad (4\text{-}2)$$

then, expanding f_i in a Taylor series in terms of the a's,

$$f_i = f_i^o + \sum_k \frac{\partial f_i}{\partial a_j} \Delta a_k \; . \qquad (4\text{-}3)$$

Substituting in (4-2),

$$\sum_i \left(z_i - f_i^o - \sum_k \frac{\partial f_i}{\partial a_k} \Delta a_k \right) \frac{\partial f_i}{\partial a_j} = 0 \; . \qquad (4\text{-}4)$$

Defining the quantities $D_{ik} = \frac{\partial f_i}{\partial a_k}$, $\Delta a_k = \Delta_k$, and $e_i = z_i - f_i^o$, equation (4-4) may be rewritten as

$$\sum_i (e_i - \sum_k D_{ik} \Delta_k) D_{ij} = 0 \; . \qquad (4\text{-}5)$$

Rearranging,

$$\sum_i e_i D_{ij} - \sum_{i,k} D_{ik} \Delta_k D_{ij} = 0 \text{ , or} \qquad (4\text{-}6)$$

$$\sum_i D'_{ji} e_i - \sum_{i,k} D'_{ji} D_{ik} \Delta_k = 0; \qquad (4\text{-}7)$$

thus, $(D' e)_j - (D' D \Delta)_j = 0$, where the quantities in parentheses are both column matrices and $D'D$ is a square matrix which should have an inverse $(D'D)^{-1}$. Multiplying through by $(D'D)^{-1}_j$,

$$(D'D)^{-1}_j D'_j e_j - \Delta_j = 0, \text{ or } \Delta_j = (D'D)^{-1} D'_j e_i . \qquad (4\text{-}8)$$

The new trial parameters are then

$$a_j^{(new)} = a_j^{(old)} + \Delta_j . \qquad (4\text{-}9)$$

The above process is repeated with the new parameters until e_i converges to a minimum and the "best" parameters may be obtained. As a measure of precision for these parameters, the standard deviations, σ_j, are calculated from

$$\sigma_j = \sqrt{\frac{\sum_i (e_i)^2}{(n-m) \sum_i (D_{ij})^2}} , \qquad (4\text{-}10)$$

where n is the number of experimental points used in the analysis and m the number of parameters to be assigned.

A least-squares analysis can be carried out using the divisions on cross-hatched paper as field intervals, but the presence of non-

linearities in the sweep limits the precision which may be attained. The best results can be obtained using frequency markers placed manually or automatically with the NMR gaussmeter system, normally at 1 kc or 100 cps intervals. With fairly stable radicals, slowing down the field sweep permits not only the enhancement of the signal-to-noise ratio, but minimization of random errors in the frequency markers as well. Maki and Volpicelli [147] point out that the approximate error in each mark is given by $\Delta f = (df/dt)\,\Delta t + \Delta f'$, where df/dt is the sweep rate, Δt is the repetition time of the frequency counter, and $\Delta f'$ is the roundoff time of the counter. Once a given sweep rate is chosen, the appropriate Δt may be chosen to minimize Δf.

An obvious shortcoming of the present program is that it fails to account for variations in linewidth within the spectrum, simply finding the best average of linewidth for all lines. As pointed out earlier, different lines within spectra occasionally have different relaxation times, thus will become power saturated at different instrumental settings and display different line widths; variations in linewidth may be found which are expressed by a quadratic equation in m_j, the total nuclear spin angular momentum, due to relaxation mechanisms arising from anisotropic intramolecular dipolar interactions between the unpaired electron and the nuclear spins and/or rotational relaxation of the anisotropic g tensor. [64] Any g tensor anisotropies which are not averaged out by rapid tumbling may lead to systematic variations in line width from low field to high, while line width alternation is often

detected when a cation may "jump" between two or more equivalent sites in the radical. A further consideration, although probably minor compared to linewidth variations, is that the sum of several Lorentzian lines is not necessarily Lorentzian. [103] , [28]

Power saturation, as well as creating linewidth variations, may affect the intensity ratios as well, making it more difficult to fit the spectrum to one calculated using the binomial coefficient intensity ratios. If the lines do not overlap too badly, severe power saturation or linewidth variations may make it advisable to revert to direct measurement of frequency differences between lines.

The least-squares program has not been designed to analyze superimposed spectra of more than one radical species.

It should be noted that complex spectra, particularly those with broad overlapping lines, may often be fit by more than one assignment of coupling constants; in addition, spectra calculated for such assignments may all resemble the experimental envelope closely. Once an assignment has been made and convergence obtained for the spectrum parameters, it is well to compare the wings of the calculated and experimental spectra to see if other assignments are possible. It may seem disappointing that a good least-squares fit of an experimental spectrum does not necessarily imply a unique assignment of the couplings, but conversely, least-squares analysis provides a more quantitative tool than the eyeball for choosing between assignments which all seem to correlate closely with the experimental data. An example of

this is the recent assignment of coupling constants made in this laboratory for the cation radical of tetramethyltetrazene (1225 theoretical lines), in which the "best" assignment was chosen from three possible cases on the basis of having the smallest residual, or best fit. [155]

The usual approach used by this worker for previously unobserved spectra was to make tentative assignments, compare the spectrum with that calculated using these tentative assignments, possibly altering parameters to obtain a closer match, then try a least-squares analysis. Once an assignment was found which produced least-squares convergence, a spectrum could be computed with the least-squared values for comparison with the experimental.

In some cases, it was found that the program failed to converge even when provided with good input parameters, if faced with a "confusing" situation such as coupling constants for different sets of nuclei being nearly equal or in an integral ratio. It was found that a "preliminary" fit could usually be obtained by combining two sets of nuclei in one "case", thus keeping the relationship between their coupling constants the same; this technique is discussed for a specific case in Section Five.

5. Results

Benzophenone

Sodium reduction of a 5 X 10^{-4} M solution of benzophenone in THF yielded a dark blue solution whose EPR spectrum (60-70 lines) resembled that obtained by Ayscough and Wilson [69] by sodium reduction in 1, 2 dimethoxyethane (DME), but displayed a reproducible asymmetry in that the hyperfine structure seemed less well resolved at the high field end. This characteristic of the spectrum was observed both in repeated sweeps with a single sample, and in observations of other samples. Coupling constants measured directly from the spectrum are given in Table 1. Further reduction normally led to a deep purple, diamagnetic solution, presumably due to the dianion. Ayscough and Wilson had reported that sodium reductions in THF or dioxane solvents often led to asymmetric EPR spectra [96] , while Hirota and Weissman [130] established through optical and EPR spectra that paramagnetic dimers (two metal cations and two anions) exist in such solutions in equilibrium with the paramagnetic monomers and other species.

Reddoch [150] has analyzed asymmetric spectra of benzophenone-lithium ketyl in DME in terms of superimposed spectra of benzophenone ketyl coupled to one or two equivalent cations, the asymmetry being introduced by a difference in g value which causes the centers of the spectra for the two species to be about 0.3 gauss apart. After initial reduction, the spectra showed interaction with one cation, but after standing several days in the presence of excess metal, the solutions

displayed spectra which indicated two equivalent counterions. Reddoch observed that the proton coupling constants were slightly larger for the species with two equivalent cations, suggesting that addition of the second counterion shifts the electron density from the carbonyl groups to the rings.

In the present study, it was not felt that the proton coupling constants for such complex spectra could be determined with sufficient precision to describe the degree of perturbation of the spin densities in the rings, and the sodium-split spectrum was not analyzed further.

Electrolysis of a .005M solution of benzophenone in THF at -2.3 V (vs. $Ag|AgClO_4$ reference electrode) gave a deep blue solution which displayed the EPR spectrum for the free anion, much like that observed by Rieger and Fraenkel [88] , though not so well resolved. Coupling constants measured directly from the spectrum are listed in Table 1.

Sodium reduction of a solution .002M in benzophenone and .044M in TBAP (TBAP/benzophenone = 22/1) gave a dark blue solution which displayed a complex EPR spectrum of moderate resolution; further reduction caused the solution to fade to light blue, and a marked reduction in line width was observed, with triplet and quartet splittings becoming resolved on even weak lines in the wings. This spectrum, shown in Figure 13 (b), was quite asymmetric, and had a total span of over 25 gauss, compared with about 20 gauss for the electrolytic spectrum. Repeated splittings about equal to the coupling constants determined from the electrolytic spectrum could be detected, but no

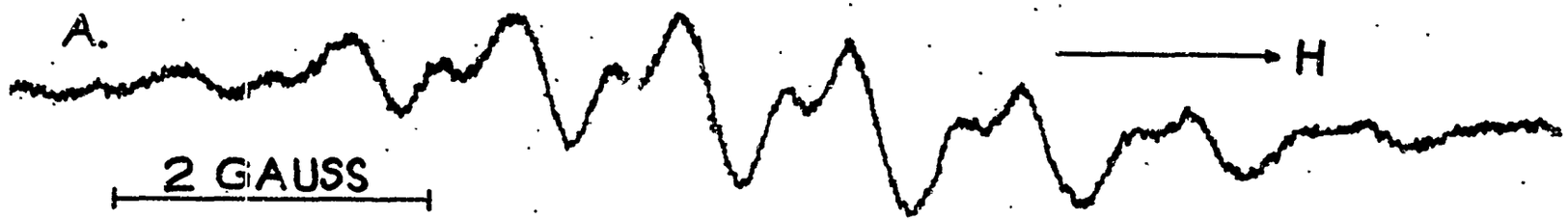

Figure 13 (a). Experimental EPR spectrum of a radical obtained by sodium reduction of hexacyanobenzene, with TBAF added.

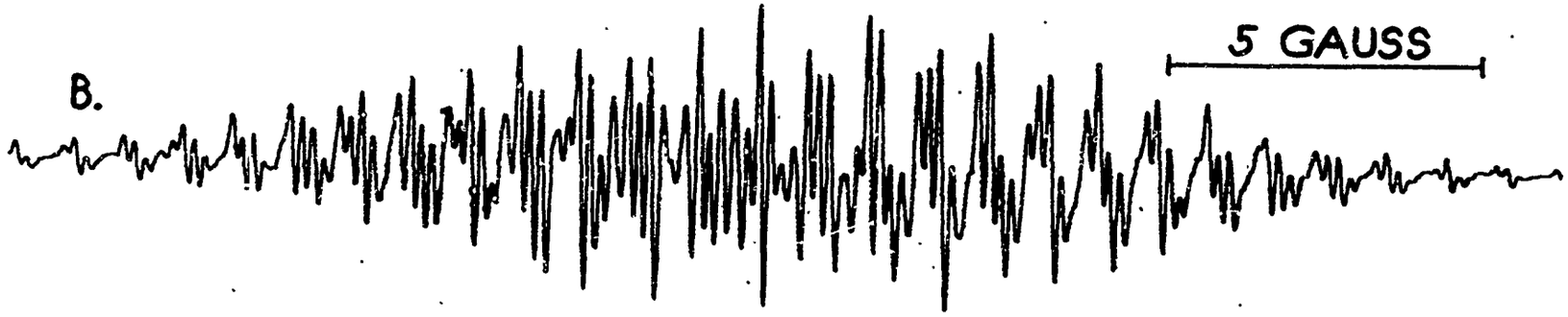

Figure 13 (b). Experimental EPR spectrum of sodium benzophenone ketyl, with TBAP added.

value which was obviously due to a sodium splitting was found. The multiplets in the wings of the spectrum and its greater span compared to the free ion spectra suggest that sodium coupling is present; the coupling constant might either be very small, splitting wing lines into multiplets, or could be nearly equal to one of the proton coupling constants. Another distinct possibility is a superposition of spectra from more than one species, such as Reddoch observed; this could account for the asymmetry and the fact that the overall pattern of the spectrum does not bear close resemblance to either the free ion or split spectra.

In this case, a particular degree of reaction with sodium made a benzophenone/TBAP sample display a marked narrowing of lines while retaining its sodium splitting or displaying some other complicating feature. The mechanism may involve some reaction of TBAP and sodium which removes species which would normally cause broadening of lines -- unreduced benzophenone or the dianion, for example.

The samples of benzophenone ketyl produced by electrolysis were generally stable for two to three hours, while well-sealed samples reduced with sodium lasted for days or longer.

Table 1. Coupling Constants for Benzophenone

Cation	a_o	a_m	a_p	a_M	Remarks
TBAP	2.52	0.83	3.54	-----	Measured.
Na^+	2.5	0.83	3.5	0.83?	Measured.

Terephthalonitrile

The yellow-orange anion radical of terophthalonitrile was obtained by electrolysis of a .002M solution at -2.1 v, the current dropping from 4.2 ma to 0.4 after about ten minutes. A solution prepared in this manner displayed an EPR spectrum of nine broad lines; following Rieger, et al. [112], an additional minute or two of electrolysis at -2.7 v resulted in more complete reduction and a well-resolved spectrum of 25 lines. Coupling constants determined by least-squares refinement of points measured directly from the spectrum are shown in Table 2, with standard deviations (thousandths of gauss) indicated in parentheses. In an attempt to introduce progressive perturbations of the ions, $NaClO_4$ was included with the TBAP electrolyte in concentrations up to 1.5 times that of terephthalonitrile. Least-square values for the coupling constants (based on points taken from a spectrum on graph paper) showed no significant variations in these cases, and no sodium coupling was observed.

This observation suggested that an abundance of TBAP might prevent sodium ions in solution from perturbing the radical anions appreciably, or producing alkali metal coupling. Indeed, reduction of a .001M solution of terephthalonitrile by a sodium mirror yielded a golden-yellow solution with an EPR spectrum of nine broad lines, further split by sodium (Figure 14); addition of TBAP in a concentration at least 25 times that of the radical removed the sodium coupling, giving a nicely resolved spectrum identical to that obtained by electrolytic

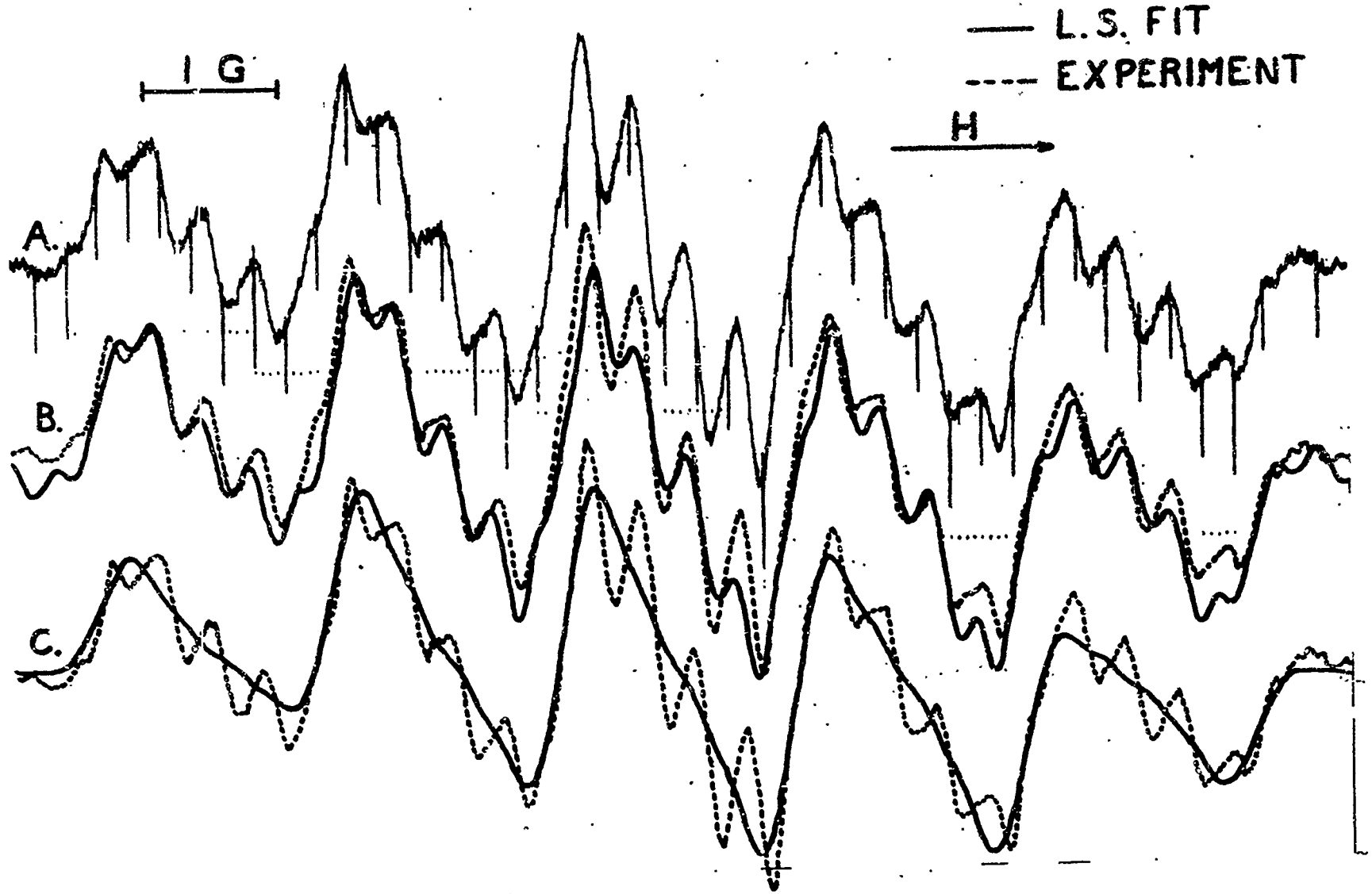

Figure 14 (a). Experimental EPR spectrum of terephthalonitrile anion radical with sodium ion; 1 kc frequency markers.
(b). Comparison of experimental spectrum (....) with spectrum calculated from least-squares refined sodium, proton and nitrogen coupling constants.
(c). Comparison of experimental spectrum with spectrum calculated from least-squares refined sodium and averaged proton/nitrogen coupling constants.

reduction. Coupling constants obtained for these two cases by least squares analysis of spectra calibrated by the NMR gaussmeter are given in Table 2. The standard deviations of the coupling constants for the sodium split case are greater than those for the "free ion" spectrum due to an apparent alternating line-width effect.

Since terephthalonitrile offers polar groups with which sodium ion should be able to form a tight complex, the radical should be more highly perturbed in the presence of sodium than in an excess of TBAP. To determine the changes to be expected in the coupling constants with greater perturbations, Hückel molecular orbital calculations were performed, using the parameters suggested by Rieger and Fraenkel [87], but neglecting overlap. The effect of the perturbing ion was simulated by altering only the Coulomb integral for the nitrogen atom, much as Gendell, Freed and Fraenkel treated solvent perturbations of the proton coupling constants of para-benzosemiquinone. [80]

Both proton and nitrogen coupling constants were observed to decrease when the radical was perturbed more strongly (i.e., Na^+ versus TBAP). This trend could be reproduced by calculations using the McConnell Q for proton splittings and equation (3-37) with the Rieger/Fraenkel parameters for nitrogen splittings. The spin density at nitrogen actually increased slightly as the perturbation was increased, so it was necessary to consider the spin densities at both the nitrile nitrogen and carbon to obtain qualitative agreement with experiment.

A solution of terephthalonitrile alone, when allowed to react with excess sodium for a day or two, yielded a blue, diamagnetic species,

which later turned lavender; solutions containing TBAP appeared to remain yellow for several days, eventually becoming colorless. Addition of TBAP in concentrations less than that of terepthalonitrile gave spectra in which the sodium splitting was better resolved than for the TBAP-free samples; accurate coupling constants have not been determined for these cases, but a sodium coupling of 0.35 gauss could easily be measured in the wings.

Figure 15 (a) shows the experimental spectrum of the terephthalonitrile anion radical prepared by reduction with sodium and addition of TBAP, with frequency markers placed every 100 cps. Figure 15 (b) is a comparison of this experimental spectrum with one calculated from least-squares refined values of coupling constants, linewidth and amplitude, the dotted lines indicating deviations of the experimental spectrum from the calculated. The fit seems quite good for the high-field portion of the spectrum, and deviations at the low-field end might be attributed to sweep non-linearities. The small peaks visible among the central lines, interpreted by Rieger, et al. [112] as C^{13} splittings, have not been considered in the least-squares analysis.

Figure 14 (a) is the central portion of the experimental spectrum of terephthalonitrile anion prepared by reduction with sodium, with 1 kc frequency markers. Figure 14 (b) and (c) are comparisons of experiment to the least-squares "fit", as above. Figure 14 (c) illustrates the fit obtained by least-squares analysis for a single average coupling constant for nitrogens and protons, plus sodium; Figure 14 (b) was

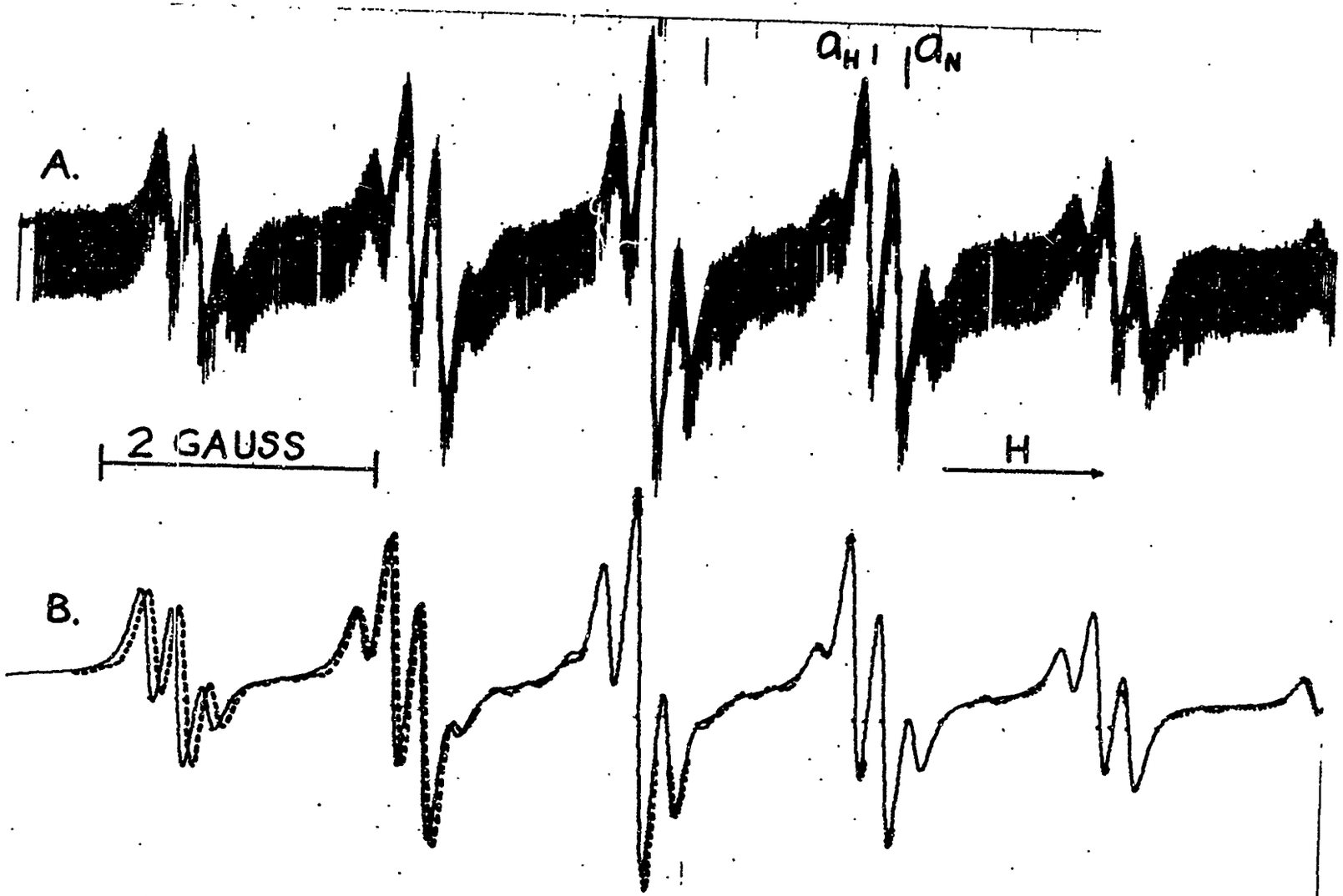

Figure 15 (a). Experimental EPR spectrum of sodium-reduced terephthalonitrile with TBAP added; 100 cps frequency markers.
(b). Comparison of experimental spectrum (....) with spectrum calculated from least-squares refined coupling constants.

obtained by using the resulting sodium coupling as a starting value for a least-squares refinement of the coupling constants for nitrogens, protons and sodium considered independently.

Carrington and Todd observed the EPR spectrum of terephthalonitrile radical prepared by reduction with alkali metals in a 3:1 mixture of DME and THF at -100 deg. C, but observed no alkali metal splittings. [100]

Table 2. Coupling Constants for Terephtholonitrile

Cation	a_H	a_N	a_M	Remarks
TBAP	1.538(7)	1.771(6)	--------	Electrolysis; L.S., std. scale.
TBAP/Na+	1.556(1)	1.781(1)	--------	TBAP added; L.S., std. scale.
TBAP/Na+	1.575(1)	1.801(1)	--------	TBAP added; L.S., 100 cps.
TBAP/Na+	1.576(1)	1.796(1)	--------	TBAP added; L.S., 1 kc
TBAP	1.521(6)	1.788(5)	--------	Electrolysis, $(NaClO_4)/(TBAP)=.75$; L.S., std. scale.
TBAP	1.560(2)	1.787(2)	--------	Same; $(NaClO_4)/(TBAP)= 1.5$.
Na^+	1.522(3)	1.771(3)	0.360(2)	L.S., 1 kc
Na^+	1.718(7)	1.718(7)	0.330(5)	L.S., 1 kc; $a_H = a_N = a$.

Anthracene

Electrolysis of a .002M solution of anthracene at -2.3 v produced a dark blue solution; upon dilution, an EPR spectrum similar to that of Bolton and Fraenkel [18] (TBAP electrolyte, DME solvent) was obtained. Coupling constants determined by direct measurement and by least-squares refinement of points taken from a spectrum on graph paper are shown in Table 3.

Reduction of .001M anthracene by sodium gave a deep blue solution which displayed a complex EPR spectrum of rather broad, overlapping lines which are apparently due to coupling by the sodium ion. (Reaction with excess sodium gave the dark blue, diamagnetic dianion.) Splitting by an additional single proton would produce a similar pattern for the central lines, but comparison of the wings of the spectrum with the "free ion" spectrum suggested that a quartet splitting was present. Coupling constants determined by least-squares analysis of NMR-calibrated spectra are shown in Table 1; the standard deviations are rather large because of apparent power saturation of the central lines of the spectrum and possible line-width variations.

Assignment of parameters was difficult in this case because of the broad, overlapping lines, while refinement of the parameters by least-squares analysis was complicated by the fact that the coupling constants for sodium and one set of four protons (a_2) differed by less than the experimental linewidth, and twice the coupling constant a_1 (four protons) was nearly equal to the value of a_9 (two protons). In such cases, the

least-squares program has been known to neither converge or diverge, but continue iterating between two or more seemingly likely combinations of parameters. This "hunting" can often be prevented by including two sets of coupling constants in one "case", thus putting constraints on some of the parameters; since the program will presently handle only four cases, this might also be useful in the analysis of systems with more than four sets of equivalent nuclei.

The experimental spectrum of sodium-split anthracene anion radical is shown in Figure 16 (a); (b) and (c) are comparisons of this spectrum with those calculated from least-square parameters, with a_2 and a_{Na} being combined in one case for (b), while no simplifications were made in (a). The residuals are very nearly equal for these two analyses (27.9 and 28.6), but the amplitudes differ by about 10%, making (b) apparently a slightly better fit.

Addition of TBAP to a prepared solution of sodium-reduced anthracene anion, or sodium reduction of a solution of anthracene and TBAP, normally gave spectra (Figure 1a) identical to those obtained by electrolytic reduction; coupling constants determined by repeated measurements of line positions with the NMR gaussmeter are shown in Table 3. Spectra computed using these coupling constants matched the experimental line positions very well, although the intensities did not compare as favorably, due to power saturation of the central lines in the experimental spectrum.

Some rather complex chemistry seems involved here, as indicated

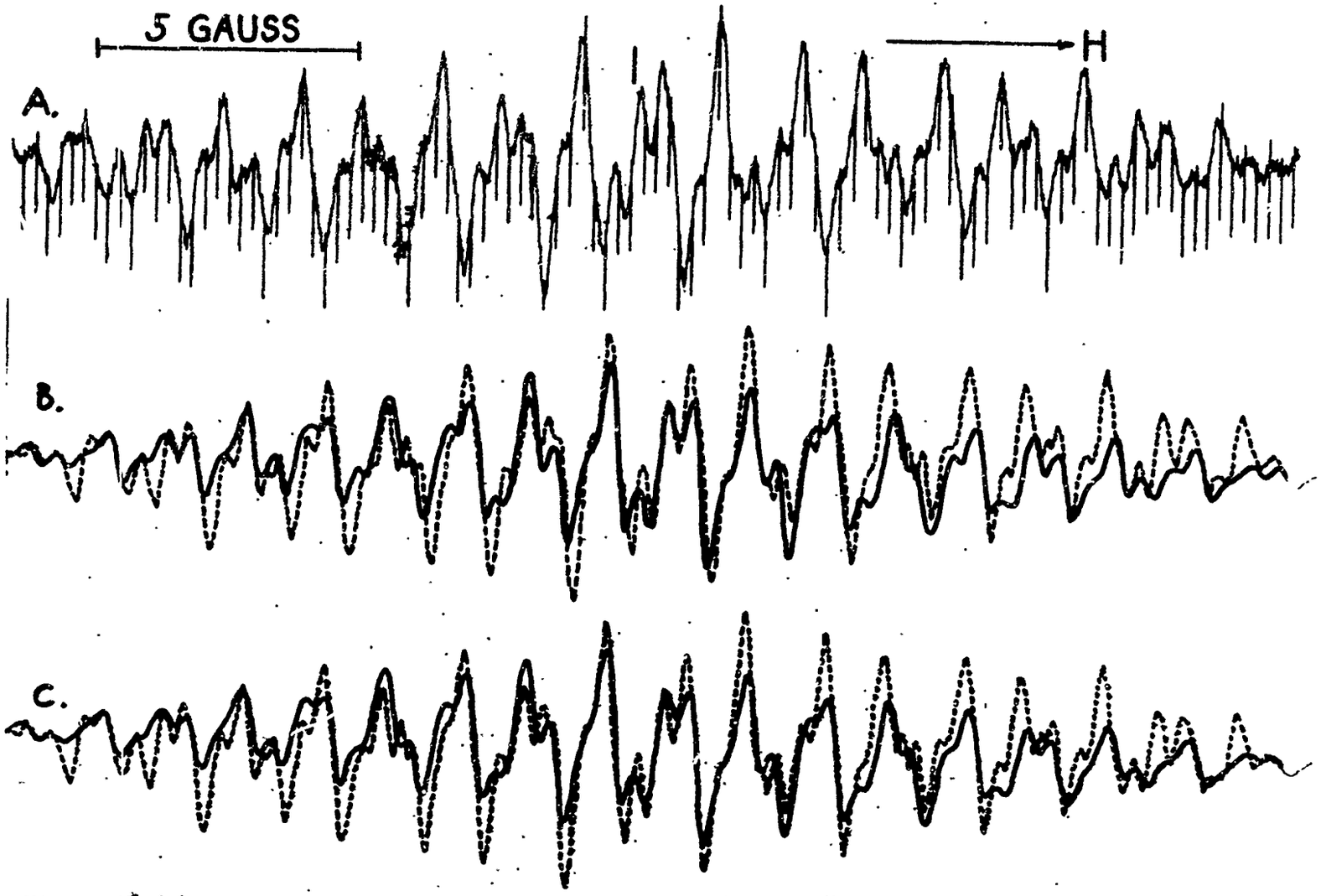

Figure 1. (a). Experimental EPR spectrum of sodium-reduced anthracene; 1 kc. frequency markers.
(b). Comparison of experimental spectrum (....) with spectrum calculated from least-squares fit for $a_{H2} = a_{Na}$.
(c). Comparison of experimental spectrum with spectrum calculated from least-squares refined coupling constants.

by an entertaining, if puzzling, display of colors. Colors appearing on the sodium mirror as it was formed included various shades of blue, red and purple. When a solution of TBAP and anthracene is reacted with sodium for a few moments at a time, it turns pale blue, then yellow, yellow-green, and finally, olive green; a dark olive green seemed to display the best spectra. The dark olive solution decayed (over widely varying time scales) to a golden yellow, diamagnetic species, which in turn became almost colorless after a few hours. This solution later turned pink, the color intensifying over a period of a day or two, before it became truly colorless. No EPR signals could be observed in the yellow, pink, or colorless solutions. Such "final decay" products could then be reacted with the sodium again, going quickly from blue to green and yellow.

No previous report has been found of the observation of sodium splitting in the spectrum of anthracene anion radical in THF. Reddoch [149] observed this radical using a variety of reducing agents and solvents, including lithium, sodium and potassium in THF, but observed cation splitting only with sodium or potassium in tetramethylenediamine (TMED) or potassium in diethyl ether (DEE). Nishiguchi, et al. [148] observed small metal splittings for anthracene in THP, using sodium and cesium.

Addition of TBAP to anthracene radical solutions in relative concentrations, TBAP: anthracene, as low as 1:2 was observed to eliminate sodium splitting, while lower concentrations produced spectra

with sodium splitting. When quantities near the minimum amount of TBAP for "sodium removal" were added, it was noted that the "split" spectra could sometimes be regenerated. The radicals often decayed to a yellow or colorless solution within hours of preparation, but further reaction with sodium produced a blue solution which displayed a spectrum with sodium splitting.

Addition of tetrabutylammonium bromide (TBAB) to anthracene radicals prepared with sodium also produced unsplit spectra, although the solubility of TBAB is very low in THF. Addition of $NaClO_4$ appeared to have no effect.

The coupling constants obtained for anthracene radical in the presence of TBAP matched a point on Reddoch's correlation diagram [149], but those for the sodium-split case were apparently not well-determined enough to allow a fit.

Table 3. Coupling Constants for Anthracene

Cation	a_1	a_2	a_9	a_M	Remarks
TBAP/Na^+	2.668( )	1.534( )	5.361( )	----	TBAP added.
TBAP	2.62	1.47	5.33	----	Measured.
TBAP	2.64	1.50	5.31	----	L.S., std. scale.
Na^+	2.607(12)	1.496(9)	5.439(13)	1.627(10)	L.S., 1 kc.
Na^+	2.626(11)	1.569(6)	5.449(13)	1.569(6)	L.S., $a_2 = a_M$.

Biphenyl

Sodium reduction of a .003M solution of biphenyl gave a medium blue radical which displayed the 45-line EPR spectrum (nine quintets) expected for biphenyl without sodium splitting. Coupling constants determined by least-squares analysis of an NMR-calibrated spectrum are given in Table 4. Since $a_1 = 2a_2$, it was necessary to include these in a single case to obtain convergence. The experimental spectrum is illustrated in Figure 17 (a), while (b) and (c) show the central portion and how it is fit by a computed spectrum. When solvent was distilled into a sample holder containing the sodium mirror and biphenyl, various colors appeared on the glass. Normally the frozen solution at the bottom of the tube turned blue; a band of pink appeared above this, followed by a band of yellow/green/blue.

Sodium reduction of a solution of biphenyl and TBAP resulted in the initial formation of the blue radical anion, which seemed to be destroyed rapidly as a yellow-orange diamagnetic species appeared. Similarly, addition of TBAP to a prepared solution of radical quickly gave the yellow diamagnetic solution.

Alkali metal splittings have been observed in the spectrum of the biphenyl radical anion for lithium, sodium, potassium, rubidium and cesium in tetrahydropyran (THP) [148] ; and for potassium in THP, 2, 3-dihydropyran, THF, and DME [135] . The metal coupling constants were of the order of 0.1 gauss for sodium, lithium and potassium. In the present study, linewidths were about 0.15 gauss, and alkali

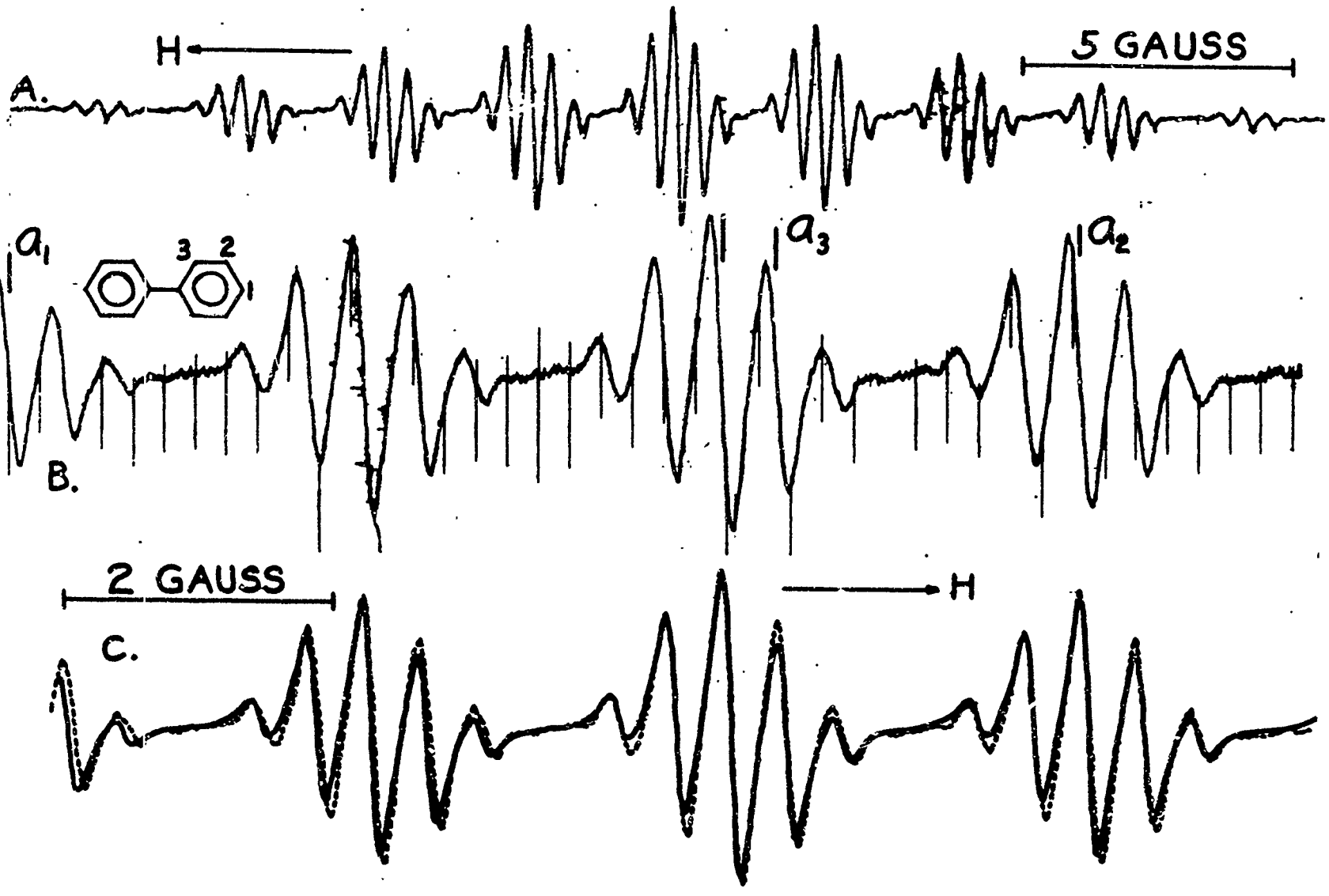

Figure 17 (a). Experimental EPR sectrum of sodium-reduced biphenyl.
(b). Central portion of biphenyl spectrum; 1 kc frequency markers.
(c). Comparison of experimental spectrum (....) with one calculated from least-squares refined coupling constants; $a_1 = 2a_2$.

metal splittings were not resolved.

It was planned to investigate any changes in the appearance of the spectrum or shifts in coupling constants as TBAP was added to a THF solution of sodium-reduced biphenyl, but the unresolved metal couplings and the rapid decay of the radical when TBAP was present discouraged this line of inquiry. However, the work did provide another example of a relatively unperturbed radical for which accurate coupling constants could be determined and a close match of computed and experimental spectra obtained. (See Figure 17 (c).)

Table 4. Coupling Constants for Biphenyl

Cation	a_1	a_2	a_3	a_M	Remarks
Na^+	5.360(4)	2.680(2)	0.413(2)	----	L.S., $a_1 = 2a_2$.

Hexacyanobenzene

A solution 8 X 10^{-4}M in hexacyanobenzene was prepared in the usual manner in a sample holder with a needle-valve sidearm containing 85 moles of TBAP per mole hexacyanobenzene. Since it was possible that visible light might cause the molecule to decompose, only light from windows on the far side of the laboratory was used for illumination, and the solution was shielded further by wrapping the sample holder in black paper. When the solution was first warmed to room temperature, a faint purple color was evident; on contact with the sodium mirror, a red reaction product formed, giving a final solution which was pink in

color. A dark precipitate also formed.

This pink solution displayed an EPR spectrum consisting of one line about four gauss wide; after dissolving the TBAP in the solution, most of the color disappeared, but the resulting solution gave the spectrum shown in Figure 13 (a). After about four hours, the radical decayed, leaving a yellowish solution.

The spectrum of nine broad lines with further splitting partially resolved on the central four is difficult to analyze in terms of the expected six equivalent nitrogens, which would produce a pattern of thirteen lines with relative intensities 1:6:21:50:90:126:141:126:90:50:21:6:1. There is no strong central line at the apparent center of the experimental spectrum, as would be predicted for all splittings due to nitrogens; a large splitting by a single sodium or proton might appear to "push the wings away from the center", however. If TBAP removes the effect of the sodium ion as it did with terephthalonitrile and anthracene, sodium splitting should not appear. Rieger, et al. [12] observed that if phthalonitrile was subjected to electrolysis in DMF solution at the potential of the second polarographic wave, one of the nitrile groups was lost, being replaced with a proton from the solvent. Although THF is probably less likely to provide protons than is DMF, the possibility of the loss of one or more nitrile groups in the presence of excess sodium should be considered. More than one set of equivalent nitrogens might result in such a case, but the various possible combinations have not been analyzed.

Since a radical anion of hexacyanobenzene with six equivalent nitrogens would have symmetry D_{6h}, further experimental work might provide an opportunity to attributethe broad lines observed to a dynamical Jahn-Teller effect. The Jahn-Teller theorem predicts that a non-linear molecule with orbital degeneracy will be unstable in a configuration having its full molecular symmetry, and will tend to distort itself into a more stable, non-degenerate configuration of lower symmetry. If the stabilization energy for this distortion is sufficiently small, the molecule may oscillate among several possible distorted configurations, producing a type of vibronic broadening of the hyperfine coupling constants.

Only one possible case of a permanent Jahn-Teller distortion has been reported -- the anion radical of tricyano-sym-triazine, prepared by reduction with alkali metals in THF, exhibits an EPR spectrum which is interpreted as due to two sets of two and four equivalent nitrogens, respectively, rather than three and three as would be expected. [139]

Broadening of hyperfine lines in EPR spectra seems to have been first attributed to the dynamical Jahn-Teller effect for the anion free radicals of corenene, triphenylene and benzene. [50] Spectra which appear to display the same effect have been observed with the anion radical of hexamethylbenzene [105] , the tropyl radical [89] , [99] and the cation radical of coronene. [54] The EPR spectra for the radical anions of sym-trinitrobenzene [126] and cyclooctatetraene [42] , [114] , however, do not appear to show any effects of Jahn-Teller distortions.

The addition of alkyl substituents [72] or deuteration [132] of benzene removes the degeneracy and the broadening of hyperfine structure.

The original theory as set forth by Jahn and Teller [2] , [3] was later applied to dynamical effects in degenerate molecules by Moffitt and Liehr [24] , [17] , Longuet-Higgins, et al. [27] , and Clinton and Rice [34] . Further applications to hydrocarbon radicals, including calculations of energy differences between the distorted and symmetrical configurations and discussions of potential energy surfaces, have been developed by McConnell and McLachlan [61] , Hobey and McLachlan [41] , McLachlan [62] , Hobey [104] , McConnell [60] , Snyder [49] , and Coulson and Golebiewski [77] .

If further observations of radicals formed by the reduction of hexacyanobenzene result in asymmetric and/or broadline spectra, it would be of interest to perform some calculations and attempt to predict whether an observable permanent Jahn-Teller distortion and/or dynamical broadening of hyperfine structure are to be expected for this molecule. Spectra could be calculated for the various combinations of equivalent and non-equivalent nitrogens which might result from a permanent distortion, then compared with experimental spectra as an aid to interpretation.

6. Conclusions

The benzophenone ketyl radical has been produced by electrolysis and by reduction with sodium in THF, giving spectra which appear identical to those previously reported. Reduction by sodium in the presence of TBAP leads to an EPR spectrum with narrow, well-resolved lines which is asymmetric, spans a greater field than that for sodium benzophenone ketyl, and has not been interpreted.

Anthracene anion radical has been produced under similar circumstances, and with TBAB in addition. The radical observed when anthracene is reduced with sodium in THF is interpreted as displaying a sodium splitting of about 1.6 gauss, with the proton coupling constants shifted only slightly; the least-squares fit is not good enough to permit assignment of definite shifts, however. Addition of TBAP or TBAB in concentrations as small as that of the radical removes the apparent sodium coupling from the spectrum, leaving it identical to that obtained by electrolysis; a yellow decomposition product is formed, but generally does not alter the stability of the radical enough to hamper observations.

Biphenyl anion radical, produced by reduction with sodium, displayed the expected EPR spectrum, but addition of TBAP before or after reaction with the sodium resulted in rapid decay of paramagnetic species, giving a final yellow, diamagnetic solution.

Terephthalonitrile anion radical was prepared by electrolysis and sodium reduction, with and without TBAP; spectra from the electrolytic reductions appear identical to those obtained by sodium reduction with

TBAP. The spectrum of terephthalonitrile reduced by sodium in THF displays a sodium splitting of about 0.36 gauss and a slight alternating-line width effect. As predicted for radicals with polar substituents, sodium ion causes greater perturbations of spin density than does TBAP. Hückel molecular orbital calculations, using parameters from the literature, predict the trends observed -- both nitrogen and proton coupling constants decrease with increasing perturbation.

The EPR spectrum of a radical obtained by reduction of hexacyanobenzene with sodium in THF and additon of TBAP has been observed, but cannot be attributed to six equivalent nitrogens. The lack of a central line of maximum intensity may be due to splitting by sodium or a single proton. The broad lines observed suggest a dynamical Jahn-Teller effect like those observed in other molecules of symmetry D_{6h}.

A search of the literature discloses increasing interest in the observation of shifts in proton and nitrogen coupling constants resulting from environmental perturbation of spin densities in radicals, and in mathematical modeling of such systematic perturbations. The directions and approximate magnitudes of such shifts can often be reproduced by the variation of Hückel parameters, by calculating the effect of a perturbing cation near the molecule, or by estimating the equilibria which exist between two or more species with slightly different coupling constants. Attempts to reproduce the shifts produced by changes in solvent composition or cation identity or concentration are of interest, but the temperature and concentration of the samples may have to be

controlled closely to make the observations meaningful. Probably the best system yet devised for comparison of theoretical predictions with experimentally observed shifts is Reddoch's empirical correlation diagram, since it permits the use of spectra obtained under widely varying conditions, thus encouraging comparison with observations in the literature.

The observed removal of sodium coupling by addition of an electrolyte is believed to be of possible utility as well as theoretical interest. In the cases of terephthalonitrile and anthracene, spectra obtained from the product of a simple sodium-TBAP reduction were identical to those produced by tedious manipulations of a complex electrolysis cell. In the cases of benzophenone and hexacyanobenzene, addition of TBAP to the sodium reduction products revealed additional structure, producing spectra which were very interesting, if not immediately interpretable as those of the "free anions".

The reasons for the removal of sodium coupling by TBAP seem to lie in its effect on the complex equilibria which exist in solutions of radicals produced by alkali metal reductions. Taking R as an aromatic hydrocarbon and T^+ as the tetra-n-butyl ammonium ion, an equilibrium which certainly exists is the following:

$$Na^+R^- + T^+ + ClO_4^- \rightleftharpoons T^+R^- + \begin{matrix} Na^+ + ClO_4^- \\ /\!/ \\ NaClO_4 \end{matrix} \qquad (6\text{-}1)$$

The loss of sodium coupling is probably caused by the removal of sodium from close association with the radical anion, rather than by an exchange process as is sometimes observed for the addition of excess alkali halide; this removal could be effected by T^+ having a greater affinity for the anion than does Na^+, and/or by Na^+ being held more strongly by ClO_4^- than by the anion. The latter possibility seems most likely, as the more localized charge of ClO_4^- should form a tighter ion pair with Na^+ than does a large hydrocarbon radical anion. Further work with the tetra-alkyl ammonium halides, acetate, etc., should be of interest in verifying this hypothesis.

The narrowing of lines without removing sodium may be due to a shift of equilibrium (6-1), or possibly to a chemical reaction which removes species which would normally broaden the lines (such as the unreduced hydrocarbon or its dianion). The chemical behavior of anthracene anion in the presence of TBAP has been most completely investigated; a reaction appears to take place in the presence of a radical solution containing TBAP and sodium, leading to a yellow decomposition product. The yellow product is observed to form upon the sodium surface when a solution of anthracene and TBAP touches it. Similar decompositions have not been observed in electrolytic preparations, where sodium is not present. No colored products formed in a solution of TBAF in THF containing a pellet of sodium which was kept under vacuum.

It is felt that TBAP (or the halides, acetate, etc.) might be well-

employed in a quantitative study of the coupling constants of hydrocarbon anion radicals, with or without polar functional groups, prepared in the presence of various ratios of alkali metal cations and the tetra-n-butyl ammonium ion. Sodium and TBAP could be used in THF, or possibly a mixed electrolyte of $NaNO_3$ and TBAP could be used for electrolytic preparations in a solvent such as DMF.

An investigation of the spectra displayed by various hydrocarbons when reduced with sodium in the presence of TBAP would be of interest, particularly in the cases of those which lose their sodium coupling and remain stable enough for careful observation. The chemical reactions which occur in the solutions remain a mystery, and should be investigated by some analytical method which will leave the evacuated tubes undisturbed. The ultraviolet-visible spectra should be of interest for comparison with the abundance of literature references on solutions of hydrocarbons, their anions and dianions, and for the observation of the radicals in the presence of a different cation than has ordinarily been used.

Acknowledgments

The author wishes to express his appreciation to Dr. William M. Tolles for the guidance and assistance he has provided throughout the progress of this research, and to the faculty members of the Department of Material Science and Chemistry who supplied enlightenment and encouragement along the way. Thanks are also due to Mr. Robert A. Sanders

for construction of the NMR gaussmeter, Mr. Jan van Gastel for his skilled glassblowing, the Computer Facility, U. S. Naval Postgraduate School for computation time, and the Office of Naval Research for partial support of the investigation.

BIBLIOGRAPHY

1. Luder, W. F. and P. B. Kraus, J. Am. Chem. Soc. 58, 255 (1936).

2. Jahn, H. A. and E. Teller, Proc. Royal Soc. A161, 220 (1937).

3. Jahn, H. A., Proc. Royal Soc. 164A, 117 (1938).

4. Holden, A. N., C. Kittel, F. R. Merritt and W. R. Yager, Phys. Rev. 77, 147 (1950.

5. Pound, R. V. and W. D. Knight, Rev. Sci, Instr. 21, 219 (1950).

6. Lipkin, D., D. E. Paul, J. Townsend and S. I. Weissman, Science 117, 534 (1953).

7. Weissman, S. I., D. E. Paul, J. Townsend and G. E. Pake, J. Chem. Phys. 21, 2227 (1953).

8. Chu, T. L. and S. C. Yu, J. Am. Chem. Soc. 76, 3367 (1954).

9. Jarrett, H. S. and G. J. Sloan, J. Chem. Phys. 22, 1783 (1954).

10. Ward, R. L. and S. I. Weissman, J. Am. Chem. Soc. 76, 3612 (1954).

11. Weissman, S. I., J. Chem. Phys. 22, 1378 (1954).

12. Venkataraman, B. and G. K. Fraenkel, J. Chem. Phys. 23, 588 (1955).

13. Venkataraman, B. and G. K. Fraenkel, J. Am. Chem. Soc. 77, 2707 (1955).

14. Wertz, J. E., Chem. Rev. 55, 829 (1955).

15. Bersohn, R., J. Chem. Phys. 24, 1066 (1956).

16. Fraenkel, G. K. and B. Venkataraman, J. Chem. Phys. 24, 737 (1956).

17. Liehr, A. D. and W. Moffitt, J. Chem. Phys. 25, 1074 (1956).

18. McConnell, H. M., J. Chem. Phys. 24, 632 (1956).

19. McConnell, H. M., J. Chem. Phys. 24, 762 (1956).

20. Paul, D. E., D. Lipkin and S. I. Weissman, J. Am. Chem. Soc. 78, 116 (1956).

21. Weissman, S. I., J. Chem. Phys. 25, 890 (1956).

22. de Boer, E. and S. I. Weissman, Rec. trav. chim. 76, 824 (1957).

23. McConnell, H. M., Ann. Rev. Phys. Chem. 8, 105 (1957).

24. Moffitt, W. and A. D. Liehr, Phys. Rev. 106, 1195 (1957).

25. Weissman, S. I., T. R. Tuttle and E. de Boer, J. Phys. Chem. 61, 28 (1957).

26. Adam, F. C. and S. I. Weissman, J. Am. Chem. Soc. 80, 2057 (1958).

27. Austen, D. E. G., P. H. Given, J. E. Ingram and M. E. Peover, Nature 182, 1784 (1958).

28. de Boer, E. and S. I. Weissman, J. Am. Chem. Soc. 80, 4549 (1958).

29. Longuet-Higgins, H. C., U. Öpik, M. H. L. Pryce and R. A. Sacks, Proc. Royal Soc. 244A, 1 (1958).

30. McConnell, H. M. and H. H. Dearman, J. Chem. Phys. 28, 51 (1958).

31. McConnell, H. M. and D. B. Chesnut, J. Chem. Phys. 28, 107 (1958).

32. Tuttle, T. R., Jr. and S. I. Weissman, J. Am. Chem. Soc. 80, 5342 (1958).

33. Carrington, A., F. Dravnieks and M. C. R. Symons, J. Chem. Soc. 1959, 947.

34. Clinton, W. L. and B. Rice, J. Chem. Phys. 30, 542 (1959).

35. Maki, A. H. and D. H. Geske, J. Chem. Phys. 30, 1356 (1959).

36. McConnell, H. M. and R. W. Fessenden, J. Chem. Phys. 31, 1688 (1959).

37. Venkataraman, B., B. G. Segal and G. K. Fraenkel, J. Chem. Phys. 30, 1006 (1959).

38. Aten, A. C., J. Dieleman and G. J. Hoijtink, Disc. Faraday Soc. 29, 182 (1960).

39. Carter, H. V., B. J. McClella and E. Warhurst, Trans. Faraday Soc. 56, 455 (1960).

40. Geske, D. H. and A. H. Maki, J. Am. Chem. Soc. 82, 2671 (1960).

41. Hobey, W. D. and A. D. McLachlan, J. Chem. Phys. 33, 1695 (1960).

42. Katz, T. J. and H. L. Strauss, J. Chem. Phys. 32, 1873 (1960).

43. Maki, A. H. and D. H. Geske, J. Chem. Phys. 33, 825 (1960).

44. McConnell, H.M., J. Chem. Phys. 33, 115 (1960).

45. McConnell, H. M., J. Chem. Phys. 33, 1868 (1960).

46. McLachlan, A. D., Mol. Phys. 3, 233 (1960).

47. McLachlan, A. D., H. H. Dearman and R. Lefebvre, J. Chem. Phys. 33, 65 (1960).

48. Schreurs, J. W. H., G. E. Blomgren and G. K. Fraenkel, J. Chem. Phys. 32, 1861 (1960).

49. Snyder, L. C., J. Chem. Phys. 33, 619 (1960).

50. Townsend, M. G. and S. I. Weissman, J. Chem. Phys. 32, 309 (1960).

51. Varian Associates, NMR and EPR Spectroscopy, Pergamon, 1960.

52. Ward, R. L., J. Chem. Phys. 32, 410 (1960).

53. Atherton, N. M. and S. I. Weissman, J. Am. Chem. Soc. 83, 1330 (1961).

54. Bolton, J. R. and A. Carrington, Mol. Phys. 4, 271 (1961).

55. Coulson, C. A., Valence, Oxford, 1961.

56. Karplus, M. and G. K. Fraenkel, J. Chem. Phys. 35, 1312 (1961).

57. Maki, A. H., J. Chem. Phys. 35, 761 (1961).

58. Maki, A. H. and D. H. Geske, J. Am. Chem. Soc. 83, 1852 (1961).

59. McClelland, B. J., Trans. Faraday Soc. 57, 1458 (1961).

60. McConnell, H. M., J. Chem. Phys. 34, 13 (1961).

61. McConnell, H. M. and A. D. McLachlan, J. Chem. Phys. 34, 1 (1961).

62. McLachlan, A. D., Mol. Phys. 4, 417 (1961).

63. Rieger, P. H., I. Bernal and G. K. Fraenkel, J. Am. Chem. Soc. 83, 3918 (1961).

64. Schreurs, J. W. H. and G. K. Fraenkel, J. Chem. Phys. 34, 756 (1961).

65. Streitwiser, A., Molecular Orbital Theory for Organic Chemists, John Wiley & Sons, 1961.

66. Vincow, G. and G. K. Fraenkel, J. Chem. Phys. 34, 1333 (1961).

67. Ward, R. L., J. Am. Chem. Soc. 83, 1296 (1961).

68. Atherton, N. M., F. Gerson and J. N. Murrell, Mol. Phys. 5, 509 (1962).

69. Ayscough, P. B. and R. Wilson, Proc. Chem. Soc. 1962, 229.

70. Bernal, I., P. H. Rieger and G. K. Fraenkel, J. Chem. Phys. 37, 1489 (1962).

71. Bolton, J. R. and A. Carrington, Mol. Phys. 5, 161 (1962).

72. Bolton, J. R., A. Carrington, A. Forman and L. E. Orgel, Mol. Phys. 5, 43 (1962).

73. Carrington, A., Mol. Phys. 5, 161 (1962).

74. Carrington, A., Mol. Phys. 5, 425 (1962).

75. Carrington, A. and H. C. Longuet-Higgins, Mol. Phys. 5, 447 (1962).

76. Carrington, A. and J. dos Santos-Veiga, Mol. Phys. 5, 21 (1962).

77. Coulson, C. A. and A. Golebiewski, Mol. Phys. 5, 71 (1962).

78. de Boer, E. and E. L. Mackor, Mol. Phys. 5, 493 (1962).

79. Freed, J. H. and G. K. Fraenkel, J. Chem. Phys. 37, 1156 (1962).

80. Gendell, J., J. H. Freed and G. K. Fraenkel, J. Chem. Phys. 37, 2832 (1962).

81. Freed, J. H., P. H. Rieger and G. K. Fraenkel, J. Chem. Phys. 37, 1879 (1962).

82. Heineken, F. W., M. Bruin and F. Bruin, J. Chem. Phys. 37, 452 (1962).

83. Hirota, N., J. Chem. Phys. 37, 1884 (1962).

84. Hyde, J. S. and H. W. Brown, J. Chem. Phys. 37, 368 (1962).

85. Pake, G. E., Paramagnetic Resonance, Benjamin, 1962.

86. Piette, L. H., P. Ludwig and R. N. Adams, J. Am. Chem. Soc. 84, 4212 (1962).

87. Rieger, P. H. and G. K. Fraenkel, J. Chem. Phys. 37, 2795 (1962).

88. Rieger, P. H. and G. K. Fraenkel, J. Chem. Phys. 37, 2811 (1962).

89. dos Santos-Veiga, J., Mol. Phys. 5, 639 (1962).

90. Stone, E. W. and A. H. Maki, J. Chem. Phys. 36, 1944 (1962).

91. Tuttle, T. R., Jr., J. Am. Chem. Soc. 84, 1492 (1962).

92. Tuttle, T. R. , Jr., J. Am. Chem. Soc. 84, 2839 (1962).

93. Ward, R. L., J. Chem. Phys. 36, 1405 (1962).

94. Aono, S. and K. Oohashi, Prog. Theor. Phys. 30, 162(1963).

95. Ayscough, P. B., F. P. Sargent and R. Wilson, J. Chem. Soc. 1963, 5418.

96. Ayscough, P. B. and R. Wilson, J. Chem. Soc. 1963, 5412.

97. Bolton, J. R., A. Carrington and P. F. Todd, Mol. Phys. 6, 169 (1963).

98. Carrington, A., Quart. Rev. 17, 66 (1963).

99. Carrington, A. and I. C. P. Smith, Mol. Phys. 7, 99 (1963).

100. Carrington, A. and P. F. Todd, Mol. Phys. 6, 161 (1963).

101. Colpa, J. P. and J. R. Bolton, Mol. Phys. 6, 273 (1963).

102. de Boer, E. and E. L. Mackor, Proc. Chem. Soc. 1963, 23.

103. Freed, J. H. and G. K. Fraenkel, J. Chem. Phys. 39, 326 (1963).

104. Hobey, W. D., Mol. Phys. 7, 325 (1963).

105. Hulme, R. and M. C. R. Symons, Proc. Chem. Soc. 1963, 241.

106. Hush, N. S. and J. R. Rowlands, Mol. Phys. 6, 201 (1963).

107. Ishizu, K., Bull. Chem. Soc. Japan 36, 938 (1963).

108. McDowell, C. A., Rev. Modern Phys. 35, 528 (1963).

109. McDowell, C. A. and K. F. G. Paulus, Mol. Phys. 7, 541 (1963).

110. Pannell, J., Mol. Phys. 7, 317 (1963).

111. Pannell, J., Mol. Phys. 7, 599 (1963).

112. Rieger, P. H., I. Bernal, W. H. Reinmuth and G. K. Fraenkel, J. Am. Chem. Soc. 85, 683 (1963).

113. Slichter, C. P., Principles of Magnetic Resonance, Harper & Row, 1963.

114. Strauss, H. L., T. J. Katz and G. K. Fraenkel, J. Am. Chem. Soc. 85, 2360 (1963).

115. Symons, M. C. R., Adv. in Phys. Org. Chem. 1, 283 (1963).

116. Atherton, N. M. and A. E. Goggins, Mol. Phys. 8, 99 (1964).

117. Blandamer, M. J., T. E. Gough, J. M. Gross and M. C. R. Symons, J. Chem. Soc. 1964, 536.

118. Bolton, J. R. and G. K. Fraenkel, J. Chem. Phys. 40, 3307 (1964).

119. Carrington, A., Ann. Rpts. Chem. Soc. 1964, 27.

120. Chambers, J. Q., III, T. Layloff and R. N. Adams, J. Phys. Chem. 68, 661 (1964).

121. Corvaja, C. and G. Giacometti, J. Am. Chem. Soc. 86, 2736 (1964).

122. de Boer, E. and E. L. Mackor, J. Am. Chem. Soc. 86, 1513 (1964).

123. de Boer, E. and A. P. Praat, Mol. Phys. 8, 291 (1964).

124. Eaton, D. R., Inorg. Chem. 3, 1268 (1964).

125. Fessenden, R. W. and S. Ogawa, J. Am. Chem. Soc. 86, 3591 (1964).

126. Fischer, P. H. H. and C. A. McDowell, Mol. Phys. 8, 357 (1964).

127. Freed, J. H. and G. K. Fraenkel, J. Chem. Phys. 41, 699 (1964).

128. Gendell, J., J. H. Freed and G. K. Fraenkel, J. Chem. Phys. 41, 949 (1964).

129. Hirota, N. and S. I. Weissman, J. Am. Chem. Soc. 86, 2537 (1964).

130. Hirota, N. and S. I. Weissman, J. Am. Chem. Soc. 86, 2538 (1964)

131. Kitagawa, T., T. Layloff and R. N. Adams, Anal. Chem. 36, 925 (1964).

132. Lawler, R. G., J. R. Bolton, G. K. Fraenkel and T. H. Brown, J. Am. Chem. Soc. 86, 520 (1964).

133. Lucken, E. A. C., J. Chem. Soc. 1964, 4234.

134. Luckhurst, G. R. and L. E. Orgel, Mol. Phys. 8, 117 (1964).

135. Nishiguchi, H., Y. Nakai, K. Nakamura, K. Ishizu, Y. Deguchi and H. Takaki, J. Chem. Phys. 40, 241 (1964).

136. Reddoch, A. H., J. Chem. Phys. 41, 444 (1964).

137. Atherton, N. M. and A. E. Goggins, Trans. Faraday Soc. 61 511 (1965).

138. Blandamer, M. J., J. M. Gross and M. C. R. Symons, Nature 205, 591 (1965).

139. Carrington, A., H. C. Longuet-Higgins and P. F. Todd, Mol. Phys. 9, 211 (1965).

140. Chambers, J. Q. and R. N. Adams, Mol. Phys. 9, 413 (1965).

141. Das, M. R. and G. K. Fraenkel, J. Chem. Phys. 42, 1350 (1965).

142. de Boer, E., Rec. trav. chim. 84, 609 (1965).

143. Gross, J. M. and M. C. R. Symons, Mol. Phys. 9, 287 (1965).

144. Johnson, C. S., Jr., and R. Chang, J. Chem. Phys. 43, 3183 (1965).

145. Land, E. J., Progress in Reaction Kinetics 3, 370 (1965).

146. Lapp, T. W., J. G. Burr and R. B. Ingalls, J. Chem. Phys. 43, 4183 (1965).

147. Maki, A. H. and R. J. Volpicelli, Rev. Sci. Instr. 36, 325 (1965).

148. Nishiguchi, H., Y. Nakai, K. Nakamura, K. Ishizu, Y. Deguchi and H. Takai, Mol. Phys. 9, 154 (1965).

149. Reddoch, A. H., J. Chem. Phys. 43, 225 (1965).

150. Reddoch, A. H., J. Chem. Phys. 43, 3411 (1965).

151. dos Santos-Veiga, J. and A. F. Neiva-Correia, Mol. Phys. 9, 395 (1965).

152. Stone, E. W. and A. H. Maki, J. Am. Chem. Soc. 87, 454 (1965).

153. Tanikaga, R., K. Maruyama and R. Goto, Bull. Chem. Soc. Japan 38, 144 (1965).

154. Hameka, H. F., Advanced Quantum Chemistry, Addison-Wesley, 1965.

155. Tolles, W. M., D. W. Moore and W. E. Thun, J. Am. Chem. Soc., to be published.

INITIAL DISTRIBUTION LIST

		No. Copies
1.	Defense Documentation Center Cameron Station Alexandria, Virginia 22314	20
2.	Library U. S. Naval Postgraduate School Monterey, California 93940	2
3.	Professor William M. Tolles Department of Material Science & Chemistry U. S. Naval Postgraduate School Monterey, California 93940	2
4.	Professor John W. Schultz Department of Material Science & Chemistry U. S. Naval Postgraduate School Monterey, California 93940	1
5.	LT James K. Poole 1830 So. Adams Street Tacoma 5, Washington	1
6.	Department of Material Science & Chemistry U. S. Naval Postgraduate School Monterey, California 93940	3

UNCLASSIFIED

Security Classification

DOCUMENT CONTROL DATA - R&D

(Security classification of title, body of abstract and indexing annotation must be entered when the overall report is classified)

1. ORIGINATING ACTIVITY (Corporate author)	2a. REPORT SECURITY CLASSIFICATION
United States Naval Postgraduate School Monterey, California	UNCLASSIFIED
	2b GROUP

3. REPORT TITLE

CATIONIC PERTURBATIONS OF SPIN DENSITIES IN ANION FREE RADICALS

4. DESCRIPTIVE NOTES *(Type of report and inclusive dates)*

Final

5. AUTHOR(S) *(Last name, first name, initial)*

POOLE, James K.

6. REPORT DATE	7a. TOTAL NO. OF PAGES	7b. NO. OF REFS
May 1966	123	155

8a. CONTRACT OR GRANT NO.	9a. ORIGINATOR'S REPORT NUMBER(S)
b. PROJECT NO.	
c.	9b. OTHER REPORT NO(S) *(Any other numbers that may be assigned this report)*
d.	

10. AVAILABILITY/LIMITATION NOTICES

11. SUPPLEMENTARY NOTES	12. SPONSORING MILITARY ACTIVITY

13. ABSTRACT

In an investigation of cationic perturbations of spin densities in anion free radicals, as disclosed by variations in proton coupling constants, the EPR spectra of anion free radicals of benzophenone, biphenyl, anthracene, terephthalonitrile and hexacyanobenzene were observed. Radicals were prepared in vacuo, using a vacuum electrolytic cell and/or sodium reductions in tetrahydrofuran solution. The spectra of the anthracene and terephthalonitrile radicals, prepared by reduction with sodium in tetrahydrofuran, displayed sodium splitting. It was observed that the coupling constants for protons and nitrogens in the terephthalonitrile radical were smaller in the presence of sodium ion than in the presence of tetra-n-butyl ammonium perchlorate. It was observed that the addition of tetra-n-butyl ammonium perchlorate to sodium-reduced solutions of anthracene or terephthalonitrile removed the sodium coupling, giving narrow-line EPR spectra identical with those obtained by electrolysis in vacuo. Coupling constants for the radicals were determined by a least-squares analysis of the envelope of the central portion of the spectrum, marking field intervals with an NMR field-tracking gaussmeter and utilizing a computer program which synthesizes an EPR spectrum when given coupling constants and other parameters. This research was carried out at the U. S. Naval Postgraduate School, Monterey, California.

DD FORM 1 JAN 64 1473

UNCLASSIFIED

Security Classification

UNCLASSIFIED

KEY WORDS	LINK A		LINK B		LINK C	
	ROLE	WT	ROLE	WT	ROLE	WT
EPR, ESR, electron paramagnetic resonance Free radicals, Spin density perturbations Vacuum electrolysis Least-squares analysis Tetrabutylammonium perchlorate, Equilibria Sodium reductions Anthracene, Benzophenone, Terephthalonitrile, Hexacyanobenzene						

INSTRUCTIONS

1. ORIGINATING ACTIVITY: Enter the name and address of the contractor, subcontractor, grantee, Department of Defense activity or other organization (*corporate author*) issuing the report.

2a. REPORT SECURITY CLASSIFICATION: Enter the overall security classification of the report. Indicate whether "Restricted Data" is included. Marking is to be in accordance with appropriate security regulations.

2b. GROUP: Automatic downgrading is specified in DoD Directive 5200.10 and Armed Forces Industrial Manual. Enter the group number. Also, when applicable, show that optional markings have been used for Group 3 and Group 4 as authorized.

3. REPORT TITLE: Enter the complete report title in all capital letters. Titles in all cases should be unclassified. If a meaningful title cannot be selected without classification, show title classification in all capitals in parenthesis immediately following the title.

4. DESCRIPTIVE NOTES: If appropriate, enter the type of report, e.g., interim, progress, summary, annual, or final. Give the inclusive dates when a specific reporting period is covered.

5. AUTHOR(S): Enter the name(s) of author(s) as shown on or in the report. Enter last name, first name, middle initial. If military, show rank and branch of service. The name of the principal author is an absolute minimum requirement.

6. REPORT DATE: Enter the date of the report as day, month, year, or month, year. If more than one date appears on the report, use date of publication.

7a. TOTAL NUMBER OF PAGES: The total page count should follow normal pagination procedures, i.e., enter the number of pages containing information.

7b. NUMBER OF REFERENCES: Enter the total number of references cited in the report.

8a. CONTRACT OR GRANT NUMBER: If appropriate, enter the applicable number of the contract or grant under which the report was written.

8b, 8c, & 8d. PROJECT NUMBER: Enter the appropriate military department identification, such as project number, subproject number, system numbers, task number, etc.

9a. ORIGINATOR'S REPORT NUMBER(S): Enter the official report number by which the document will be identified and controlled by the originating activity. This number must be unique to this report.

9b. OTHER REPORT NUMBER(S): If the report has been assigned any other report numbers (*either by the originator or by the sponsor*), also enter this number(s).

10. AVAILABILITY/LIMITATION NOTICES: Enter any limitations on further dissemination of the report, other than those imposed by security classification, using standard statements such as:

(1) "Qualified requesters may obtain copies of this report from DDC."

(2) "Foreign announcement and dissemination of this report by DDC is not authorized."

(3) "U. S. Government agencies may obtain copies of this report directly from DDC. Other qualified DDC users shall request through

_____."

(4) "U. S. military agencies may obtain copies of this report directly from DDC. Other qualified users shall request through

_____."

(5) "All distribution of this report is controlled. Qualified DDC users shall request through

_____."

If the report has been furnished to the Office of Technical Services, Department of Commerce, for sale to the public, indicate this fact and enter the price, if known.

11. SUPPLEMENTARY NOTES: Use for additional explanatory notes.

12. SPONSORING MILITARY ACTIVITY: Enter the name of the departmental project office or laboratory sponsoring (*paying for*) the research and development. Include address.

13. ABSTRACT: Enter an abstract giving a brief and factual summary of the document indicative of the report, even though it may also appear elsewhere in the body of the technical report. If additional space is required, a continuation sheet shall be attached.

It is highly desirable that the abstract of classified reports be unclassified. Each paragraph of the abstract shall end with an indication of the military security classification of the information in the paragraph, represented as (TS), (S), (C), or (U).

There is no limitation on the length of the abstract. However, the suggested length is from 150 to 225 words.

14. KEY WORDS: Key words are technically meaningful terms or short phrases that characterize a report and may be used as index entries for cataloging the report. Key words must be selected so that no security classification is required. Identifiers, such as equipment model designation, trade name, military project code name, geographic location, may be used as key words but will be followed by an indication of technical context. The assignment of links, roles, and weights is optional.

DD FORM 1 JAN 64 1473 (BACK)

UNCLASSIFIED
Security Classification